INSTITUTO SUPERIOR TÉCNICO
Universidade Técnica de Lisboa

Implementation of an index to measure the depth of anaesthesia in animals

Ricardo da Costa Figueiredo
(Licenciado)

Dissertação para obtenção do grau:

Mestre em Engenharia Biomédica

Comité de Avaliação

Presidente:	Prof. Doutora Patrícia Margarida Piedade Figueiredo
Orientador:	Prof. Doutor Bertinho Manuel Andrade da Costa
Co-orientador:	Prof. Doutor Fernando Martins do Vale
Vogáis:	Prof. Doutor Agostinho Cláudio Rosa

Dezembro de 2010

Agradecimentos

No finalizar deste ciclo gostaria de começar por agradecer toda a dedicação, paciência, tolerância e simpatia do meu orientador, Professor Bertinho Andrade da Costa. Sempre procurou ajudar-me e deu me a liberdade para cometer os meus erros e com eles aprender a ser melhor. Ao Prof. Doutor Fernando Martins Vale pela disponibilidade e apoio prestado à realização deste trabalho.

Queria também agradecer o suporte financeiro do INESC-ID e da Funcação para a Ciência e Tecnologia (FCT), através da atribuição da bolsa integrada no projecto *IDEA - Integrated Design for Automation of Anaesthesia*, com referência PTDC/EEA-ACR/69288/2006. No mesmo sentido agradeço também ao investigador principal do projecto, Professor João Miranda Lemos, bem como a toda a equipa que me orientou e forneceu os dados sem os quais não poderia ter elaborado esta dissertação de mestrado.

Mas ao longo de estes 23 anos, 6 meses e 12 dias, muitas pessoas passaram pela minha vida e cada uma á sua maneira me marcou sendo também por elas e para elas que escrevo este trabalho.

Queria prestar um especial tributo ao meu avô que marcou fortemente a minha personalidade. A sua honestidade e a sua dedicação aos outros sempre foi um modelo para mim.

Às minhas avós que sempre me mimaram.

Aos meus pais pelo carinho, pela compreensão e especialmente pela educação, não esquecendo o ”*paitrocínio*”da minha formação.

Ao meu irmão que através dos seus exemplos aprendi e cresci. Às minhas peludinhas Bessy e Maggie que me incutiram o sentimento de responsabilidade de cuidar de alguém.

À Sónia que foi o meu pilar na fase mais dificil da minha vida e a quem ainda devo um pedido de desculpa.

À Rita Primavera que me ajudou a resolver alguns fantasmas.

À Diana com quem partilhei bons momentos.

A lista estender-se-ia e para não faltar ninguém vou enumerar os grupos.

Aos Estarolas, aos Amorfos, ao pessoal da natação, do liceu, da associação, da comissão, do IST. Todos vos fazem parte de quem sou e por isso este trabalho também é vosso.

Muito obrigado.

Ricardo da Costa Figueiredo

Resumo

Os recentes desenvolvimentos científicos e tecnológicos foram aproveitados pela Medicina na renovação de técnicas terapeuticas e de diagnóstico e ajudando a ultrapassar dificuldades, tais como o controlo da profundidade de anestesia.

A importância deste controlo prende-se com a necessidade de evitar que um paciente ganhe consciência durante a cirurgia podendo ficar com graves perturbações psicológicas. Actualmente existem métodos de identificação da profundidade anestésica baseados na actividade neuromuscular e na actividade electroencefalográfica.

Nesta dissertação, pretende-se analisar diferentes métodos baseados na electroencefalografia de forma a identificar qual o mais indicado à anestesia animal.

Para a análise dos índices foram usados dados previamente adquiridos de ratos e coelhos numa experiência as doses de anestético administrado variavam ao longo do tempo, mudando a profundidade anestésica.

Dos métodos analisados o Spectral Edge Frequency 95% e o Permutation Entropy ambos corrigidos com o factor de Burst Suppression, bem como a análise da distribuição de potências entre as bandas típicas do electroencefalograma apresentaram os melhores resultados.

A informação extraída através do método Shannon Entropy não distingue todos os estados, apenas o de maior profundidade, enquanto que o Approximate Entropy não identificou qualquer estado.

Os métodos comparativos são dependentes da base de dados.

Palavras-chave: Monitorização, Electroencefalografia, Profundidade de Anestesia, Entropia, Análise Espectral, Distribuição de Amplitudes

Abstract

The Medicine has used the new technological and scientific to update the diagnosis and therapeutics techniques that aid to overcome some difficulties, like the control of the depth of anaesthesia.

This control is very important because it was observed in patients that had episodes of awareness during anaesthesia dealt with some psychological trauma. Nowadays there are different methods for the identification of the depth of anaesthesia based on neuromuscular activity and electroencephalographic activity.

In this thesis, different methods based on the electroencephalography are analyzed in order to identify the best suited for animal anaesthesia.

The analysis of the approached indexes used a set of pre-acquired data from rats and rabbits in an experiment where the concentration of the anaesthetic drug changed and so the depth of anaesthesia changed too.

The best analyzed methods were Spectral Edge Frequency 95% and Permutation Entropy both corrected with a Burst Suppression Ratio, as well as the power distribution among the typical brain waves.

The information acquired through the Shannon Entropy method was unable to identify every state, however it distinguished the deeper one, while the Approximate Entropy did not recognize any.

The comparative methods are dependent on the data base used.

Keywords: Monitoring, Electroencephalography, Depth of Anaesthesia, Entropy, Spectral Analysis, Amplitude Distribution

Contents

Agradecimentos iii

Resumo v

Abstract vii

Acronyms xix

List of Symbols xxi

1 Introduction 1

1.1 Motivation 1

1.2 State of the Art 2

1.3 Thesis Description 2

1.4 Contributions of the Thesis 3

2 Nervous System 5

2.1 Histology 5

2.2 Anatomy and Function 7

2.3 Central Nerve System 8

2.4 Neural Communication 11

2.4.1 Resting Membrane Potential 12

2.4.2 Action Potential 13

2.4.3 Nerve Impulse Conduction 13

2.4.4 Synaptic Transmission 14
2.4.5 Neurotransmitters 15

3 Anaesthesia **17**

3.1 Introduction 17
3.2 Stages of Anaesthesia 18
3.3 Anaesthetics Mechanism of Action 20
3.3.1 Isoflurane 22
3.3.2 Propofol 22
3.4 Assessment of the Depth of Anaesthesia 23

4 Electroencephalography **27**

4.1 Electroencephalogram Acquisition 28
4.2 Brain Waves 29
4.3 Analyzing the EEG 31

5 Analyzed Methods **33**

5.1 Methods 34
5.1.1 Permutation Entropy 34
5.1.2 Shannon Entropy 36
5.1.3 Approximated Entropy 36
5.1.4 Spectral Edge Frequency 37
5.1.5 Spectral Edge Frequency (SEF) and Permutation Entropy (PE) corrected for burst suppression ratio 38
5.1.6 Band Distribution 39
5.1.7 Two Limit States 40
5.1.8 Finding the Similar State 42
5.2 Analysis of the Algorithms 42

6 Experimental Procedures & Results **45**

6.1 Rat Experiment 45

6.1.1 Data Acquisition . . . 46
6.1.2 Algorithm Implementation . . . 46
6.1.3 Results . . . 48
6.2 Rabbit Experiment . . . 51
6.2.1 IoC-View . . . 52
6.2.2 Procedure . . . 53
6.2.3 Results . . . 53

7 Conclusions **57**
7.1 Conclusions . . . 57
7.2 Future work . . . 58

Appendix **63**

A Rabbits Results **65**
A.0.1 Rabbit 1 . . . 65
A.0.2 Rabbit 2 . . . 65
A.0.3 Rabbit 3 . . . 66
A.0.4 Rabbit 4 . . . 67

B Implemented Code **71**
B.1 Simulation . . . 71
B.2 Burst Suppression Ratio . . . 78
B.3 Permutation Entropy . . . 79
B.4 Shannon Entropy . . . 80
B.5 Approximate Entropy . . . 81
B.6 Spectral Edge Frequency . . . 82

List of Tables

3.1 Ramsey Sedation Scale 24

4.2 Typical distribution of brain waves in different states of consciousness. 30

4.3 Typical brain waves in different levels of anaesthesia.[22] 32

5.4 Presentation of the different analyzed methods 34

5.5 Conditions to identify a specific state of anaesthesia. [22] 40

5.6 Run-time and time complexity analysis. 43

6.7 Amount of anaesthetic drug administered. 53

List of Figures

2.1 Representation of a typical motor neuron, [32] 6

2.2 Global structure of the nervous system, [32]. The other mammals exhibit the same type of structure. 8

2.3 Human Central Nervous System (CNS). It is composed by brain and the spinal cord. (©Healthwise, Incorporated) 9

2.4 Separation of the brain into four lobes, [32]. 10

2.5 The homunculus represents an human body where the proportion of the body is equivalent to the dedicated area 11

2.6 Layers of protection of the brain. 12

2.7 Action Potential. 14

2.8 Comparison between the two types of impulse conduction. On the right side the saltatory conduction, on the other the continuous conduction, [32] 15

2.9 Representation of the synaptic cleft. 16

3.10 This pictures represents the Guedel's signs for ether anaesthesia. It represents the muscle tone, breathing patterns and eye movements of each stage. [8] 19

3.11 Schematic representation of γ-aminobutyric acid type A $(GABA)_A$ receptor. 21

3.12 2D structure of propofol. 23

4.13 Representation of the nervous tissue and the electrical conduction of the signal. The triangular cells represent the glia cells while the other represent the neuron. The signal observed at the surface of the scalp is a combination of the both individual signal with some dissipation of its power. 27

4.14 Schematic representation of the electrode placement in human electroencephalography. The even numbers are placed in the right hemisphere while the odd numbers in the left. This type of the distribution of the electrodes allow to study the anatomical activity of the brain. 28

4.15 Schematic representation of the sources of noise along the ElectroEncephaloGraphy (EEG) acquisition. The EEG signal is corrupted with biological noise from the muscular activity, eye movement, with electrode artifacts like variations of the skin impedance, with electromagnetic noise brought from the electric power lines, and in the digital ElectroEncephaloGram (EEGram) there are also some noise from the discretization while converting analog to digital signal. 29

4.16 Representation of the typical EEG waves [20]. 30

4.17 This is an illustration of the observable differences in the EEGram while the anaesthesia is induced. 31

5.18 Schematic representation of a monitor index. This figure represents the generic method of predicting Depth of Anaesthesia (DoA) based in the EEG signal 33

5.19 Schematic of the motifs used to catalog the EEG changes in time domain. 35

5.20 Schematic of the motifs used to catalog the EEG changes in time domain. 35

5.21 The discrete EEG acquire a finite number of points to register the brain activity. The relation between points may be analyzed and find different types of motifs according to the number of motifs used. 36

5.22 The blue area represents 95% of the power of the signal and at its edge the SEF95. 37

5.23 The signal is separated with this block of filters with no gain. The pass-band filters have its limits set to identify the typical brain waves. 39

5.24 The function h is a bijective function. In this case it is assumed that the system evolves monotonically and so the function h as to be monotonic too. 41

6.25 Experimental set-up 46

6.26 Graphics of the whole data acquired, the global evolution of the EEG signal and the dose of isoflurane given to the rat. 47

6.27 Initial state. Top - time segment window, middle - spectral density power, bottom - histogram of amplitudes. 47

6.28 Deep anesthetized state based with a deep burst suppression. 48

6.29 Intermediate anesthetized state with burst suppression. 48

6.30 Representation of the variations of the concentration of isoflurane along time. . . . 49

6.31 Plot of the index predicted with the Band Distribution (BD) method. 49

6.32 Presentation of the index predicted with the $SEF_{95\%}$ method in purple, and the Spectral Edge Frequency corrected with Burst Suppresion Ratio (SEFBS) method in light blue. 49

6.33 Presentation of the index predicted with the Approximate Entropy (ApEn) method in blue, and the Shannon Entropy (ShEn) method in red. 50

6.34 Presentation of the index predicted with the PE method in yellow, and the Permutation Entropy corrected with Burst Suppresion Ratio (PEBS) method in black. . . 50

6.35 Presentation of the index predicted with Two Limit States (TLS) method using the histogram as feature. 50

6.36 Presentation of the index predicted with TLS method using the power spectrum distribution as feature. 51

6.37 In the picture the experimental set up is presented. The rabbit was already anaesthetized. 51

6.38 The IoC-View®monitor is a little bit bigger than a common mobilephone. In the screen it plots the EEG and the predicted index. 52

6.39 The IoC-View®monitor is connected to the patient with a cable with three leads. . 52

6.40 The electrodes are placed as illustrated in this picture, the red electrode in the center of the forehead, the yellow in the right side of the forehead and the green on in the cheek bone. 52

6.41 Representation of the variations in the rate flow of the propofol. 54

6.42 Empirical assessed of DoA. 54

6.43 In this plot DoA predictions are the IoC-View® is presented in red and the BD index is in tones of green. 54

6.44 This plot represented the indexes calculated with the $SEF_{95\%}$ with and without the correction factor of the Burst Suppression Ratio (BSR). 55

6.45 This plot represented the indexes calculated with the ApEn and ShEn methods. . . 55

6.46 This plot represented the indexes calculated with the PE with and without the correction factor of the BSR. 55

6.47 Plot with the index calculated with the IoC-View® and with the Finding Similar State (FSS) method. 56

6.48 In this picture, the TLS method is presented using two different features, in black the histogram and in yellow the power spectral distribution. 56

A.49 Results obtained with the data acquired from the first rabbit. 66

A.50 Results obtained with the methods that use a database for the data acquired from the first rabbit. 67

A.51 Results obtained with the data acquired from the second rabbit. 68

A.52 Results obtained with the methods that use a database for the data acquired from the second rabbit. 68

A.53 Results obtained with the data acquired from the third rabbit. 69

A.54 Results obtained with the methods that use a database for the data acquired from the third rabbit. 69

A.55 Results obtained with the data acquired from the fourth rabbit. 70

A.56 Results obtained with the methods that use a database for the data acquired from the fourth rabbit. 70

Acronyms

AEP	Auditory Evoked Potentials
ANS	Autonomic Nervous System
ApEn	Approximate Entropy
BD	Band Distribution
BIS	Bispectral index
BSR	Burst Suppression Ratio
CNS	Central Nervous System
DoA	Depth of Anaesthesia
EEG	ElectroEncephaloGraphy
EEGram	ElectroEncephaloGram
EMG	ElectroMyoGraphy
ENS	Enteric Nervous System
FSS	Finding Similar State
GABA	γ-aminobutyric acid type A
ICU	Intensive Care Unit
IV	Intravenous
MAAS	Motor Activity Assessment Scale
MAC	Minimal Alveolar Concentration
NMB	NeuroMuscular Blockade
NMDA	N-methyl D-aspartate
NT	Neurotransmitters
OAAS	Observer's Assessment Alertness/Sedation Scale

OR	Operating Room
PDF	Probability Density Function
PE	Permutation Entropy
PEBS	Permutation Entropy corrected with Burst Suppresion Ratio
PNS	Peripheral Nervous System
PSI	Patient State Index
RASS	Richmond Agitation Sedation Scale
RSS	Ramsey Sedation Scale
SEF	Spectral Edge Frequency
SEFBS	Spectral Edge Frequency corrected with Burst Suppresion Ratio
ShEn	Shannon Entropy
SNS	Somatic Nervous System
TLS	Two Limit States

List of Symbols

$N_{PEmotifs}$	Number of different motifs used in the PE algorithm
R	Constant of the perfect gases
T	Absolute temperature
F	Faraday's constant
n_{points}	Number of points used to define motifs in PE algorithm
H_{PE}	Entropy value calculated with PE algorithm
p_{iPE}	Probability of finding the motif i selecting random set of consecutive points
$x_{\{1,2,3\}}$	Amplitude value of three consecutive points
$N_{ShEnpoints}$	Length of the signal used in the ShEn algorithm
p_{ShEni}	Probability of picking randomly a point with amplitude in the interval i
m	Length of each pattern used to calculate ApEn
Sn	Sequence of observation
$sn(i, j + k)$	Point from the subsequence of observation i or j
P_m	Vector containing all the possible patterns
$p_m(i)$	Pattern used in the calculation of ApEn
C_{im}	Probability of finding a similar pattern to pattern $p_m(i)$
C_m	Mean value of C_{im}
n_{im}	Number of similar patterns
$vect_{power}$	Norm of the difference between the power distribution of the EEG and the database
$power_{dist}$	Power distribution among the typical brain waves
$database_i$	Vector with the power distribution of the state i

Chapter 1

Introduction

1.1 Motivation

With the development of signal data acquisition and processing technology as well as the development of mathematical tools for modeling and identification of biological systems, the horizons of its applications were broadened and its use for automatic control emerge naturally.

Wisely, medicine took advantage of these progresses and nowadays it is characterized by the intensive use of computerized equipments. A good example is the practice of anaesthesia where critical decisions are taken according to the information gathered from the clinical inspection of the patient and from the information given by those equipments. Great efforts have been done to produce tools to monitor the DoA and developing pharmacokinetics and pharmacodynamic models. Hopefully, these developments will reduce the incidence of awareness during anaesthesia, which is a serious complication with possible long-term psychological complications [19].

The introduction of autonomous controlling systems in procedures that require anaesthesia reduces the workload of the anaesthetist and allows a higher focus on the supervision of the patient stability. Moreover, in animal surgery is ordinary that the surgeon plays the role of anaesthetist with costs on the quality of the supervision of the animal which leads to a higher risk of mortality in animal anaesthesia [12]. There are several monitors used to help the evaluation of human patient state, like the NeuroMuscular Blockade (NMB) index and DoA indexes, such as BIS, Narcotrend, PSI and IoC-View, however none of those is calibrated to animal anaesthesia and in order to reduce this risk of mortality it is urgent to develop better methods to calculate the DoA in animals.

This dissertation intend to fill this gap with the development of a reliable algorithm that predicts

the DoA in animals.

1.2 State of the Art

Since the birth of anaesthesia the control and monitoring of the patient has been changing with the evolution of technology. With some primitive methods the DoA was assessed through some clinical tests. These tests consisted on the instruction of verbal commands or the infliction of painful stimulus to analyze the responsiveness, the level of anxiety and the level of analgesia of the subject. In order to standardize the relation between a level of anaesthesia and the clinical signs some scales were developed like Ramsey Sedation Scale (RSS) [27], Observer's Assessment Alertness/Sedation Scale (OAAS) [6]. Some of these scales are used both in the controlling of DoA and to measure of the anxiety levels in the Intensive Care Unit (ICU) [29]. Although the efforts made, the examinations of the patient was still a subjective method of analysis, since the anaesthetist is unable to reproduce the same tests every time he executes it and between different anaesthetists there are distinct perceptions. In order to reduce this variability, some different information is acquired, like heart rate variability, blood presure, ElectroMyoGraphy (EMG) and EEG signals. With these new data the control of the DoA was less subjective and more accurate.

Nowadays, the goal is to generate an index the defines the DoA based on the data provided by the EMG and EEG. The NMB level is assessed with the EMG, although it provides with great accuracy the level of paralysis, the information about levels of analgesia or hypnoses is none. The EEG data stores more information about the states of consciousness of the patient. There are different approaches to assess the DoA and so there are different commercial monitors that analyze features of time and frequency domain. The most common approaches used in the analysis of the EEG consist in bispectral index [31], calculation of entropy values[1], comparison with reference states [34] and evoked potentials [11].

1.3 Thesis Description

After this introduction that motivates and states the theme of this work, the thesis evolves to the chapter 2 where a characterization and description of the human model of the nervous system is presented with a summary of its histology, anatomy and function. The nervous systems is the fundamental target organ during an anaesthesia and it is very similar among all mammals and so the human model is valid for animals. Then, in chapter 3 it is presented the anaesthesia, the

evolution of the methods used to control the DoA, a brief explanation of the mechanisms of action of the anaesthetic drugs with a special focus on isoflurane and propofol and the anaesthetics used in this work. To conclude this chapter, the different stages of anaesthesia are analyzed and correlated with its clinical evidences. The chapter 4 is dedicated to present the EEG, to review its history, to identify the acquisition methods and procedures and to introduce the typical brain wave divisions and the information that can be extracted from them both in diagnosis and in control of anaesthesia.

These 3 chapters concluded the theoretical basis of the thesis and in the chapter 5 a mathematical description of the methods used to calculate the DoA based on the EEG data is presented. The used methods analyze the features extracted from the EEG signal and map them to an index with the use of mathematical tools. The functions used were different expressions of entropy, ShEn, ApEn and PE, methods to calculate the SEF. The indexes calculated with PE and SEF were corrected with the BSR. An empirical method analyzed the brain waves distribution according to the description done in [22] that defines the evolution of this distribution with the deepening of the level of DoA. Finally, an other empirical approach of assessment of the DoA was also considered by the comparison of the feature of the acquired data with a database of features of the different levels of the DoA.

The chapter 6 describes the two experiments and the results gathered, the first experiment used a rat as subject and the second 5 rabbits. The description of each procedure is made with the presentation of the objectives of the experiment, the designation of the equipment used, the techniques applied to extract and register the EEGram, and also the identification of the database constructed for the comparison methods. The evolution of the calculated indexes is analyzed against the variation of amount of the administered anaesthetic drug and in the experiment with the rabbits the indexes are also compared with the commercial monitor IoC-view and the clinical analysis, the results are presented and discussed.

Finally, in chapter 7 the main conclusions of this thesis are drawn and some future work to improve the control of anaesthesia is pointed out.

In appendix the implemented algorithms are shown and the results of four rabbits are presented too.

1.4 Contributions of the Thesis

The objective of this thesis is to develop, compare and improve some methods used in the identication of the DoA and apply them to animal anaesthesia. This study aims to launch the expansion

of new systems of control the animal anaesthesia so the workload of the veterinary may be reduced which allows him to focus on the procedure and so the risk of mortality will be reduced. Moreover, with a tighter control of the anaesthesia the doses of anaesthetic drugs used would be reduced, therefore the costs of the procedure will decrease as well as the recovery time of the animal like it occurs in human anaesthesia when a monitor is used [23] [25].

Chapter 2

Nervous System

This chapter presents the main target system of the profound general anaesthetic drugs, the nervous system. The knowledge of its anatomy, physiology and its functioning is vital to understand why the control of anaesthesia may be accomplished with the analysis of the variations of the activity of the nervous system in particular the electrical activity of the brain, EEG.

The nervous system consist in a network of specialized cells, neurons, that are for the transmission of information and signals between every part of the body. It is the *control center* of most living being, capable of several functions of vital importance. It acquires information from the inside and outside of the body and it processes, memorizes and reacts to them in order to maintain the homeostasis and the comfort of the being.

2.1 Histology

Although the functioning of the nervous system is very complex, its tissue has only two types of cells, neurons and glia [14]. The basic units that process the information are the neurons, which are specialized for nerve impulse conduction and Neurotransmitters (NT) liberation and reception. They are responsible for most of the unique functions of the nervous system. This cells are protected, supported and nourished by glia cells that promote the homeostasis of the interstitial fluid that baths them. In vertebrates, the nervous system has 10 to 50 times more glia cells than neurons. Oppositely to neurons, glia cells are capable to multiply and divide in mature system, filling the voids left by injured or diseased neurons. There are 4 types of glia cells in the CNS, astrocytes, oligodendrocytes, microglia and ependymal cells, and 2 different types founded only in

Peripheral Nervous System (PNS), Schwann cells and satellite cells [32]. Astrocytes are responsible for maintaining proper chemical environment for nerve communication, supplying nutrients and removing overmeasure neurotransmitters. They also aid the formation of the blood-brain barrier. Oligodendrocytes produce a holder network and a sheath of myelin around axons of the CNS. The function of microglia is protecting nervous cells from diseases swallowing microbes, it also migrate to injured areas in order to clear away debris of dead cells. The ependymal cells align the cavities of the brain, form cerebrospinal fluid and assist in its circulation. In the PNS, the Schwann cells help on the regeneration of axons and on the production of the myelin sheath around them. Finally satellite cells hold neurons in ganglia.

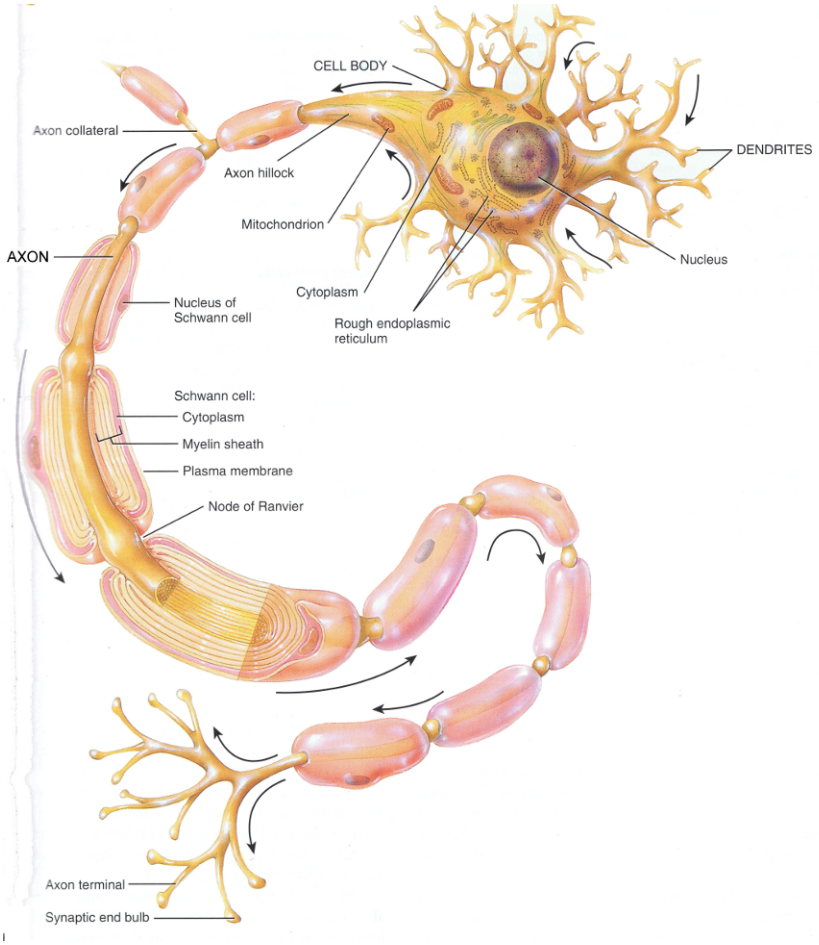

Figura 2.1: Representation of a typical motor neuron, [32]

The morphology of the neurons is very specific and well adjusted to their function. From the body cell, axons and dendrites grow. These components of the neurons allow them to communicate between different cells. Dendrites branch, with a shape of a tree, have the main function of acquiring signals and report it to body cell. The transmission of electrochemical signals is done

by axons. The axons have a linear shape with a length that goes from 0.1 mm to 2 m spreading out in the end establishing synapses, regions of communication. The majority of the axons are enfolded by a myelin sheath, a multi-layered cover of lipids and proteins, mimicking the insulation cover of an electrical wire, allowing faster nerve impulse conduction. The myelin sheath is not continuous throughout the axon, there are gaps called nodes of Ranvier.

2.2 Anatomy and Function

From all the roles of the nervous system, the more complex and intriguing activities belong to the CNS, where the memory, feelings, thoughts and reasoning are created. Due to its complexity, the comprehension of its processing is still unclear.

The nervous system is composed by two subsystems, CNS and PNS. The CNS corresponds to the brain and the spinal cord, the remaining nervous tissue belongs to the PNS.

The brain is protected by the skull and contains around 10^{11} of neurons. From the base, in mammals, twelve pairs of cranial nerves emerge. A nerve is a group of hundreds to thousands of axons surrounded by connective tissue and blood vessels that lie outside the CNS, each one goes through a well defined path, enervating a specific region of the body. Enclosed by the bones of the vertebral column is the spinal cord which contains about 100 million neurons, from where thirty-one pair of spinal nerves rise to a particular place. Sensory receptor may be dendrites of sensory neurons or separated and specialized cells that monitor changes in the internal or external environment.

The nervous system is responsible for vast and complex group of tasks like detecting different smells, speaking, producing and recalling memories, controlling movements and promoting the homeostasis. These activities can be separated in three function groups: sensory, integrative and motor. The sensory functions like sensing an increase of body temperature or a touch are detected by sensory receptors and the information is carried to the brain by sensory or afferent neurons. The integrations, the processing of the sensory information is analyzed and stored so that the responses become more appropriate. There are specific neurons to these functions, the interneurons, whose axons are short. The responses to the integrative decision create the motor function. The neurons dedicated to this function are motor or efferent neurons. The cells and organs that interact with these neurons are defined as effectors. Skeletal muscle fibers and glands cells are examples of effectors.

A different way to classify the nervous system, according to the consciousness of the action produced, divides the system in 3 groups: Somatic Nervous System (SNS), Autonomic Nervous

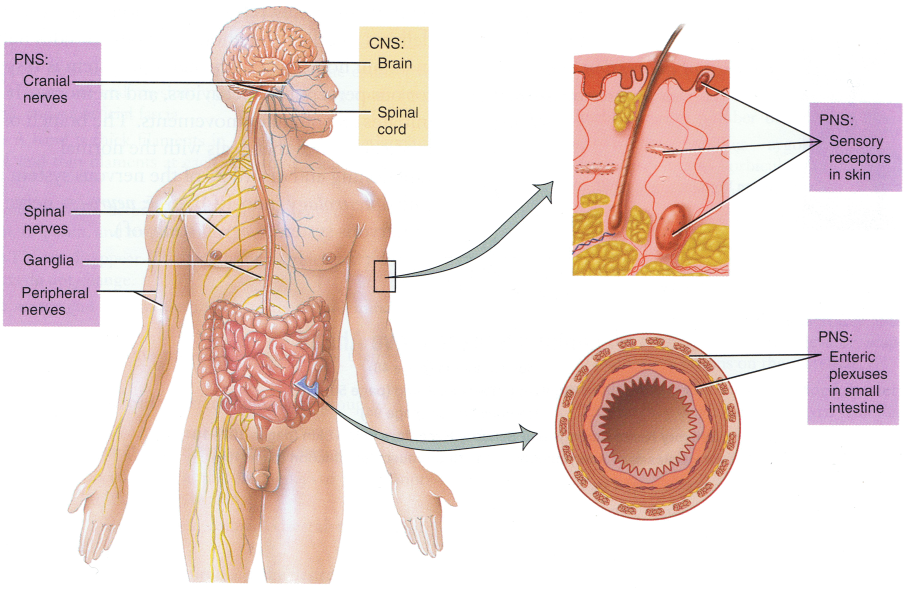

Figura 2.2: Global structure of the nervous system, [32]. The other mammals exhibit the same type of structure.

System (ANS) or Enteric Nervous System (ENS).

SNS (somat - body) acts on expression of conscious sensations and voluntary movements.

ANS (auto - self and -nomic - law) consists on the autonomic sensations and involuntary actions, enervating structures like smooth muscle, heart and glands. These actions are always “paire” with its antagonist and so it is divided into sympathetic and parasympathetic neurons. The first is responsible for the “fight or flight” actions, whereas the parasympathetic activates “rest and digest” actions.

The “brain of the gut” is played by the ENS, capable of controlling the gastrointestinal system even when it is separated from the rest of the nervous system.

2.3 Central Nerve System

As it was said before, the spinal cord and the encephalous compose the CNS. The spinal cord is a group of neurons and glia cells, disposed with a cylindrical shape inserted in the spinal column. It emerges from the base of the skull (where it is connected to the medulla oblongata), going to the lumbar region of the column. Along its path, some spinal nerves emerge enervating a specific region. It primary function is transmitting the neural signal between the brain and the rest of the body, using its ascendent and descendent fibers. The spinal cord can be divided in two parts, the grey matter and the white matter. The grey matter has essentially the body cells of the neurons

whereas the white matter is predominantly nerve fibers.

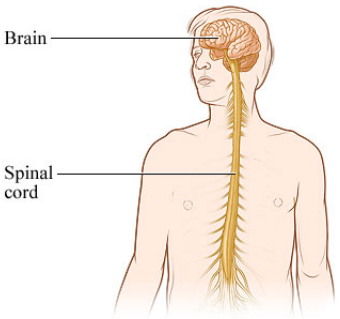

Figura 2.3: Human CNS. It is composed by brain and the spinal cord. (©Healthwise, Incorporated)

The encephalous is located in the cranial cavity and it is the center of the nervous system for almost every animal. In order to simplify and relate clearly the anatomic structure of the brain, it can be divided into three parts: brainstem, brain and cerebellum.

The brainstem is located beneath the brain and the cerebellum, divided in three components: medulla oblongata, pons and mesencephalon. The medulla oblongata corresponds to the ending of the spinal cord into the skull. In this structure, a decussation can be found, the motor and sensitive cells from one side cross to the other side, leading to a contralateral processing of the information. The pons connects the brain to diencephalon. It is located on the superior region of the brainstem and it is the biggest component. Finally, the mesencephalon is caudally and frontally adjoined to the pons and diencephalon respectively. It has an important role in motivation and habituation in every animal due to the production of dopamine from its substantia nigra.

The cerebellum lays on the posterior region of the skull, behind the brainstem and below the occipital lobs of the brain, where a fold of dura matter separates them. A group of fibers called cerebral pedunculus connects it to the rest of the CNS. As the names show, in Latin *(*cerebrum) means brain, the cerebellum and the brain have a similar structure. They both are divided in hemispheres, cortex, medulla and have folds and. It plays a fundamental role in coordination and smoothness of movements, analyzing and correcting the information sent to the motor neurons.

The brain, the main part of the encephalous, might also be divided in two sections, diencephalon and telencephalon. The first one is symmetric and has special structures like the thalamus, responsible for the integration of sensory stimulus, the hypothalamus, the central controller of the ANS, regulation the body temperature, circadian cycles, sensations like hunger, thirst and satiety, the subthalamus, which controls the muscular activity, and the epithalamus, important in the regulation of the reproductive metabolism. At last, the telencephalon is divided in two

hemispheres with some grooves and circles on its surface. Its cortex is formed by a gray matter and its interior by white matter. The variation of shade is due to the high number of myelinated axons in the white matter, while the gray matter has a great concentration of neuron body cells. Each hemisphere can be subdivided in four lobes with the same name as the cranial bone that protect them: frontal, parietal, temporal and occipital. Their frontiers are the sulcus that separates them, central sulcus cut apart the frontal and the parietal lobes, the lateral sulcus, also known as Sílvio's fissure, detach the frontal and parietal from the temporal and finally the parieto-occipital sulcus define the lobes that named it.

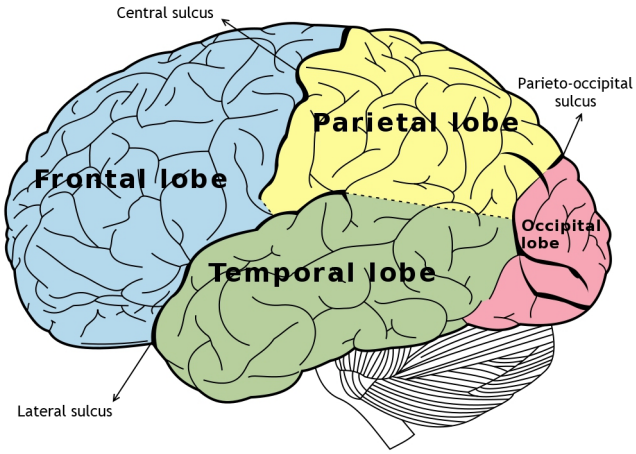

Figura 2.4: Separation of the brain into four lobes, [32].

It is well known that the functions played by the nervous system is a result of a complex and vast neuron communication and sometimes with neurons that are apart. However, in an effort to simplify, some functions are attributed to specific regions of lobes. In this way, a *functional map* of an healthy brain can by studied.

Then the posterior region of the frontal lobe is electrical stimulated some movements in the contralateral body arise and so this area is named primary motor. Some specific areas can be identified for the activity of some particular parts of the body. Scientific society thinks that the other region of the frontal lobe, pre-frontal cortex, has a important role on the definition of the personality of the subject.

The parietal lobe has regions dedicated to acquire and process sensory information. A primary section, where a map of the body can by built like in the primary motor area, is located on the anterior region. It receives the information that is then processed in the secondary section that interprets the texture, shape and size of the touched object. In both primary sensory and motor areas the regions related to each part of the body can be found. The homunculus of these two functions are represented in figure 2.5.

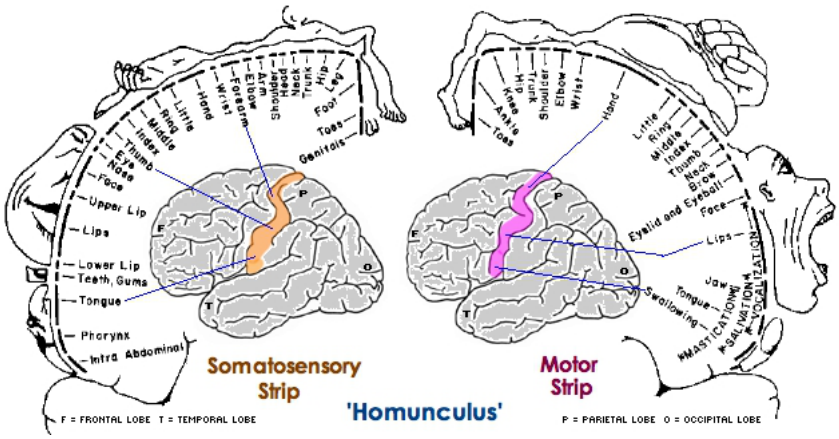

Figura 2.5: The homunculus represents an human body where the proportion of the body is equivalent to the dedicated area

Similarly to the parietal lobe and the sensory complex, the occipital lobe is mostly dedicated to the processing of the vision. In a median area the primary section is located, acquiring the signal sent from the retina. In the surrounding area the data received is processed and compared with the passed experiences, allowing the object recognition.

Finally, in the temporal lobe the audition is the main occupation. Sound of different frequencies activate different regions of the contralateral temporal lobe. There are also two different regions, one that gets the stimuli and the other which interprets them.

The connection between the lobes is accomplished by the white matter fibers. The greatest and most important structure of this communication is the corpus callosum, located underneath the lateral sulcus.

Three membranes, named pia mater, arachnoid mater and dura mater, protect the brain. Between the first two, in the subarachnoid space, flows a fluid called the cerebrospinal fluid, which nourishes the brain and let it float avoiding potential mechanical trauma caused by impacts with the skull. The liquid is colorless with glucose, some lymphocytes and a saline concentration similar to the blood plasma.

2.4 Neural Communication

The communication between neurons and neurons with muscles fibers depends on nerve action potentials, nerve impulses, and release of NT. The induction of these impulses require two basic features of plasma membrane, the membrane must have specific types of ion channels and there must be a resting membrane potential. The membrane potential is the difference between the

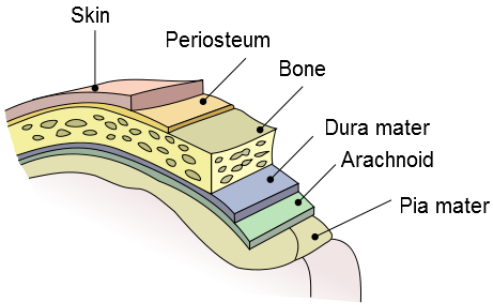

Figura 2.6: Layers of protection of the brain.

global electric charge on the inside and the outside of the cell, when it is different from zero is said to be polarized. While it is not conducting, the voltage across plasma membrane of muscle fibers and neurons is called the resting membrane potential, the inside is negatively charged, while the outside is positively charged. This is possible because the phospholipid bilayer membrane is impermeable to ions, and so in order to allow the flow of ions, creating electrical currents, some membrane proteins create pores forming specific ions channels.

There are two kinds of ion channels, leakage channel that allows a small but regular flow of ions to leak across the membrane, this type of channel has a specific affinity to different ions. At a rest stage, while the membrane is polarized, the membrane's permeability to K^+ is much higher than to Na^+ because there are many more channel of K^+ than Na^+. Another type of channels are gated channels, which open and close in response to specific stimulus. Voltage-gated channels react to changes in membrane potential and are used to generate and conduct action potentials. While others, in synaptic transmission, react to the binding of some specific ligands, like NT.

2.4.1 Resting Membrane Potential

While a neuron is in a resting state, the outside of the membrane is positively charged and the inner side is negatively charged, creating the resting membrane potential which, in neurons, is about -70mV.

This potential emerge from the different concentration of various ions in interstitial fluid and cytosol. The cytosol is rich in K^+ ions, however, the presence in higher quantity of negatively charged ions of phosphates liked to organic molecules and amino acids of proteins turn this environment in a global negatively charged. On the other hand, the interstitial fluid has higher concentration of Na^+ and Cl^-. The membrane potential is a function of the concentration and membrane's permeability to each ion according to Goldman-Hodgkin-Katz voltage equation [13], eq. 2.1

$$V_{resting} = \frac{RT}{F} ln \frac{P_K[K^+]_{out} + P_{Na}[Na^+]_{out} + P_{Cl}[Cl^-]_{in}}{P_K[K^+]_{in} + P_{Na}[Na^+]_{in} + P_{Cl}[Cl^-]_{out}}, \quad (2.1)$$

where R is the constant of the perfect gases, T absolute temperature and F is the Faraday's constant.

2.4.2 Action Potential

The action potential occurs after a sequence of rapid events that change reversibly the potential of the membrane potential returning to the resting state. Muscle fibers and neurons have the ability to convert stimuli into action potentials, this is named electrical excitability. Action potentials follow the all-or-none principle and so, if the stimulus can depolarize the membrane over a threshold value, then an action potential is generated in two phases: a depolarizing phase and a repolarizing phase. While in the depolarizing phase, a decrease and a possible change in the polarization of the membrane happens, turning the inside more positive than the outside. After that, the membrane polarization is restored to the resting state during the repolarizing phase. These two phases of an action potential last about one millisecond.

During the depolarization phase, when the potential of the membrane passes the threshold value two types of voltage-gated ions channels are opened. In neuron cells, these channels are focused in the axon and axon terminal membranes. The first type of gates opened is the Na^+ channel which allows the inflow o Na^+ ions, changing the membrane potential from $0mV$ to $+30mV$. The other type of gates are the voltage-gated K^+ channels that open more slowly and let the K^+ ions leave the cell,making the repolarizing phase. The outflow of K^+ may be greater than enough leading to after-hyperpolarizing phase. In the end the membrane potential returns to the resting level around $-70mV$.

2.4.3 Nerve Impulse Conduction

The propagation of nerve impulses along the neuron starts usually in the axon hillock and then travels to the axon terminal, along the axon. This movement evolves by positive feedback and is called conduction or propagation. At the axon hillock a depolarization opens voltage-gated Na^+ channels, with the consequent inflow of Na^+ the adjacent membrane is depolarized to threshold, opening its channels, this is the positive feedback effect. Thus, the impulse is regenerated keeping its amplitude along the axon.

The speed of the impulse conduction varies if the axon is myelinated or not. In the first type of

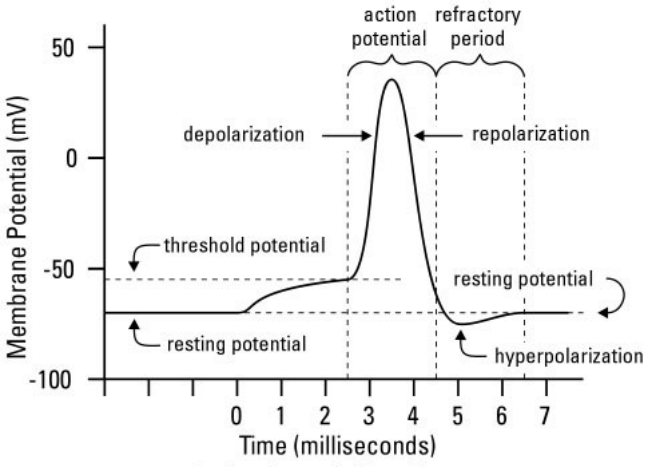

Figura 2.7: Action Potential.

axon, the faster one, the conduction is saltatory. In this neurons, the voltage-gated ionic channels are located primarily in the gaps of the myelin sheath, the nodes of Ranvier. While conducting, the current flows through the intersticial fluid that surrounds the myelin sheath to the next node. The impulse at the first node generates a current that opens the Na^+ channels at the second node, triggering the impulse there. This process travels along the axon in every consecutive node.

With a different mechanism the propagation is accomplished in unmyelinated axons with the plasma membrane depolarization to threshold and creates an action potential that depolarizes the adjacent segment. This process repeats from the body cell to the axon terminals and is called continuous conduction.

The speed of impulse conduction is function essentially of the presence or absence of a myelin sheath and the diameter of the axon. Other variables like temperature influence too.

2.4.4 Synaptic Transmission

The communication between neurons or neurons with effectors is accomplished by a series of events called synaptic transmission. The neuron transporting the impulse is known as the presynaptic neuron and the one receiving it the postsynaptic neuron. Although these two neurons are tight at a synapse, their membranes do not touch and the space between them is the synaptic cleft that is filled with interstitial fluid. Since the impulses cannot pass across the synaptic cleft an indirect form of communication is used.

When a nerve impulse get to the end of the axon, the presynaptic axon, the depolarizing phase

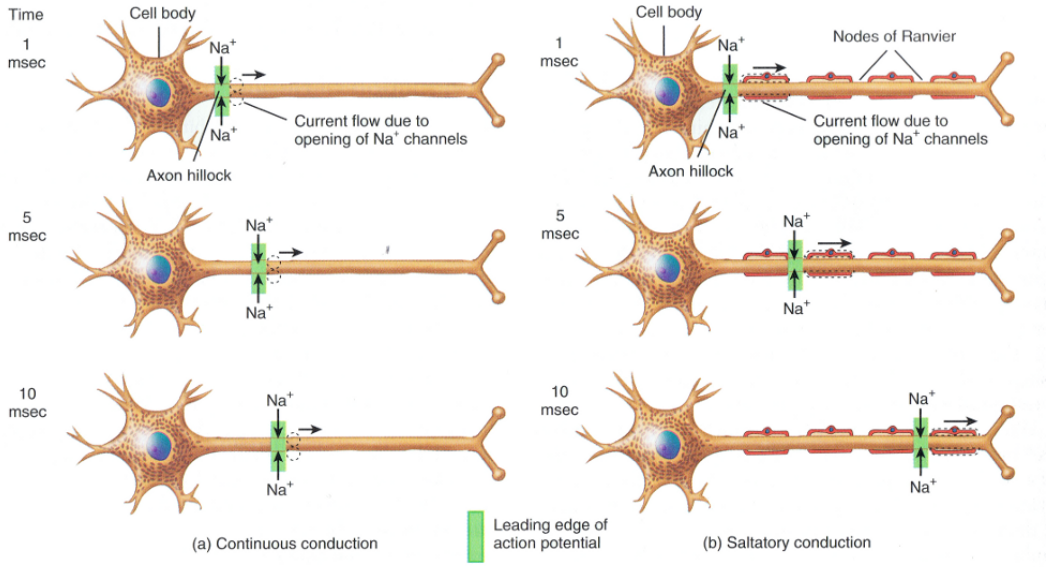

Figura 2.8: Comparison between the two types of impulse conduction. On the right side the saltatory conduction, on the other the continuous conduction, [32]

opens the Ca^{2+} channels and since its concentration is higher in the interstitial fluid, the ion flows into the presynaptic terminal. The increase of the inside concentration of Ca^{2+} triggers the exocytosis, releasing thousands of neurotransmitter molecules to the synaptic cleft. In the postsynaptic neuron, neurotransmitters receptors when associated with their ligand induce may open some ion channels and so allowing the inflow of ions, or activating some enzymes potentiating some cellular activities, starting the propagation of the information. At most synapses the information is transferred in one direction only.

2.4.5 Neurotransmitters

After the discovery of the gap between neurons, the synaptic cleft, the possibility of electrical synaptic communication started to be doubted. With the work of the German pharmacologist Otto Loewi, in 1921, the neuron communication was confirmed to be a chemical process, mediated by neurotransmitters.

In [7] the term neurotransmitter is defined as “a substance (such as norepinephrine, acetylcholine, or dopamine) that is released from the axon terminal of a presynaptic neuron on excitation, and that travels across the synaptic cleft to either excite or inhibit the target cell”. These endogenous chemicals are transported in synaptic vesicles before the arrival of the action potential that releases the neurotransmitters to the synaptic cleft.

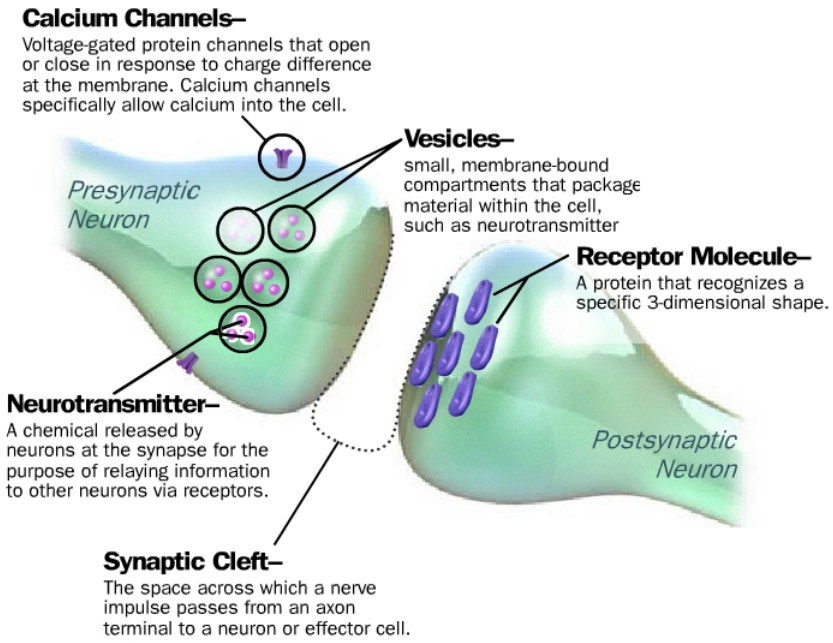

Figura 2.9: Representation of the synaptic cleft.

The neurotransmitters can be divided according to its chemical structure into amino acids, peptides and monoamines. The most common are serotonin, dopamine, epinephrine, also known as adrenaline, and norepinephrine. Although the neurotransmitters effect directly the receptors on postsynaptic cells, their action may be either excitatory or inhibitory.

When an anaesthetic drug interacts with these elements of the neural communication, the information that was supposed to reach a specific place in the nervous system is blocked and so its function is suppressed. This is the principle of the anaesthesia that is presented with some detail in the following chapter.

Chapter 3

Anaesthesia

During a procedure that may cause pain and distress, like surgery, the patient must be unconscious. This reversible condition with lack of awareness is called general anaesthesia, this word is formed from the Greek, *an-*, “without”, and *aisthésis*, “sensation”.

Analgesia, hypnosis, amnesia and paralysis are supposed to be induced to achieve general anaesthesia. While in this condition, the patient will not be able to feel pain or generate memories, the surgeon is capable to line up the patient properly and the reactive movements and autonomic reactions from the CNS will be suppressed.

As it was said before, the anaesthesia is a reversible state of consciousness induced with the administration of specific drugs that interact with the nervous system. This chapter presents a brief description of anaesthesia and its evolution, the different states of anaesthesia, the mechanisms of action of the anaesthetic drugs focussing in the ones used in the experiments, isoflurane and propofol. The control and assessment of the DoA is discussed in this chapter too.

3.1 Introduction

Unlike the different areas of medicine, the anaesthesia has almost no therapeutical nor diagnostic purpose. The development of anaesthesia techniques and anaesthetics drugs is based on three main goals:

1. Minimizing the unwanted and dangerous effects of anaesthesia;
2. Keeping the homeostasis, the healthy balance of the body, under the procedure;
3. Improving the recovery of the patient.

The induction of general anaesthesia affects all the systems of the being and the outcome of these effects indicates the DoA. Some of the physiological changes as the lowering of the blood pressure, the obstruction of the airways, the relaxation of the esophagus with probability of regurgitation and hypothermia are evidences of the dangerous effects of the anaesthesia. While recovering, some patients present nausea symptoms and may also vomit. To minimize these adverse symptoms the DoA must be controlled in order to use the minimal doses of the administrated anaesthetic drug, and so it is needed to recognize the different stages of anaesthesia.

3.2 Stages of Anaesthesia

The general anaesthetics are a group of drugs that induces general anaesthesia, which may be observed as a state of global but reversible depression of the CNS that leads to the loss of perception and responsiveness of all the external stimuli. The state of anaesthesia is assessed through the collection of different behavioral and perceptive changes of the patient. The effects and the goals of the general anaesthesia are:

1. Amnesia, the patient is unable to form memories;
2. Analgesia, the patient can not feel pain;
3. Immobility and suppression of reactive movements and autonomic reaction;
4. Loss of awareness.

In the beginnings of anaesthesia the induction was accomplished with only one drug, ether. Back then, the patient that was anaesthetized passed through four distinct observable stages where the third of these stages is subdivided into four *substages* / planes. Although nowadays the induction of surgical anaesthesia is accomplished with a combination of different drugs, each of them attains each objective of anaesthesia, and so some of the classical stages are suppressed, the same classification may still useful. Despite the differences between the anaesthesia induced with ether or with a combination of anaesthetic drugs, this classification provides a background for understanding the evolution of the anaesthesia. The new techniques and the different anaesthetic drugs allow the use of less amount of drugs and so there is a minimization of its inconveniences and hazards.

Figure 3.10 presents the different levels of breathing patterns, muscle tone and eye movement expected in each stage of anaesthesia.

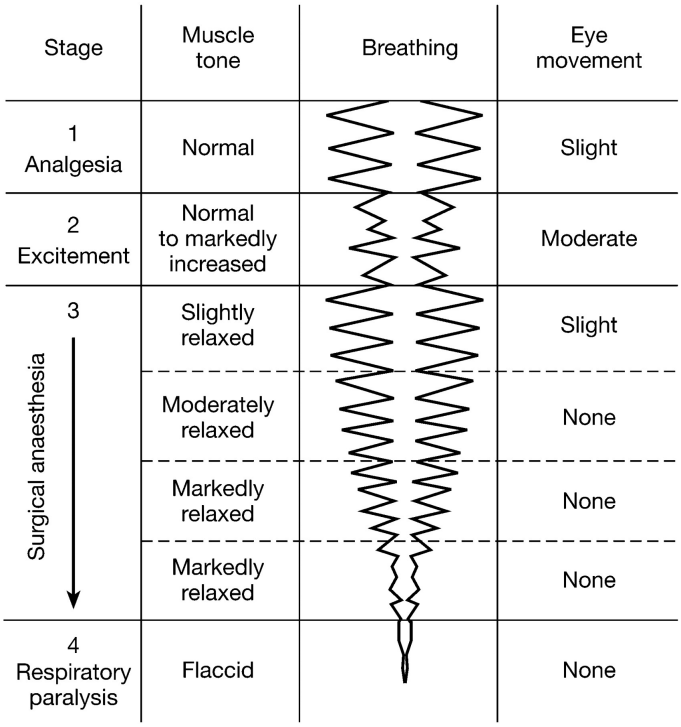

Figura 3.10: This pictures represents the Guedel's signs for ether anaesthesia. It represents the muscle tone, breathing patterns and eye movements of each stage. [8]

In the first stage, analgesia is partial, the consciousness and sense of touch are retained while the sense of hearing is increased. In the second stage, the patient may enter in a state of delirium, he is unconscious but some autonomous movements may be observed. The patient may also shout senseless word and become violent. These two stages are hardly noticed when the anaesthesia is induced with recent techniques.

The third stage, surgical tolerance, is divided in four different *substages*/planes with increasing depths with increasing levels of depression of the breathing. The depth of each *substage* depends on some characteristic changes in respiration, pupil dilation, spontaneous eyeball movements, reflexes and muscle tone.

The last and unwanted stage is called medullary paralysis and it is an anaesthetic accident, with a high risk of death. The newer anaesthetics and its combination in the induction of anaesthesia have rendered some of the signs less reliable [8].

3.3 Anaesthetics Mechanism of Action

The mechanisms of action of these drugs have been one of the greatest mysteries of pharmacology. In the early XX century, a theory of a common mechanism was widely accepted, it was said that all the anaesthetic drugs acted in the same way through interactions with the membrane of the cell. This theory was supported with the correlation of the anaesthetic power and its solubility in organic solvent, olive oil, This is the rule of Meyer-Overton and it indicates that the interaction site should be in the cellular membrane that is mainly a phospholipid bilayer membrane. However, some exceptions of the rule were observed, some anaesthetic drugs with identical physical properties had their own kind of effects. And so, this perception led to some speculation about the existence of different mechanisms and different action sites that stands that the anaesthetic drug should interact with specific proteins. This led to the abandonment of the unitary theory.

It is known that the anaesthetic drugs disable some functions of the nervous system and it is obvious that the anatomical interaction site of the general anaesthetics must be in the nervous system both in the peripheral sensory neurons, spinal cord, brainstem and the cerebral cortex. It is hard to define the exact interaction site since the anaesthetic drug inhibits the electrical activity of the CNS in diffuse way.

At cellular level, the inhaled anaesthetic drugs hyperpolarize the neurons and the probability of the generation of action potentials is reduced in response of the liberation of neurotransmitters. In higher concentrations, the inhaled anaesthetics block the synaptic transmission and have also some effects on the generation and propagation of the electric signal. These anaesthetic drugs inhibits the excitatory synapses and excites the inhibitory synapses and lead to the depression of the nervous system.

Differently, the Intravenous (IV) anaesthetic drugs act directly on the synapses where they interact with specific neurotransmitters. The great majority of these anaesthetics intensifies the inhibitory neurotransmission, the exception is ketamine that interacts with the excitatory transmission, blocking it in the glutamatergic synapses.

Many inhaled and IV anaesthetic drugs bind to $GABA_A$ receptors, controllers of the chloride channels, this bound raises the sensibility to the GABA, which leads to the inhibition of the nervous system. None of the general anaesthetic drugs competes with GABA for its binding site. These IV anaesthetic drugs are $GABA_A$ receptor agonists.

The $GABA_A$ receptor agonists modulate the receptor positively, delaying the closure of the ion channel. The $GABA_A$ receptor is a transmembrane receptor composed by different glycoprotein subunits that mold a chloride channel. In vivo, the receptor is a pentameric complex of α, β and

γ, arranged as $\alpha\alpha\beta\beta\gamma$[16], figure 3.11.

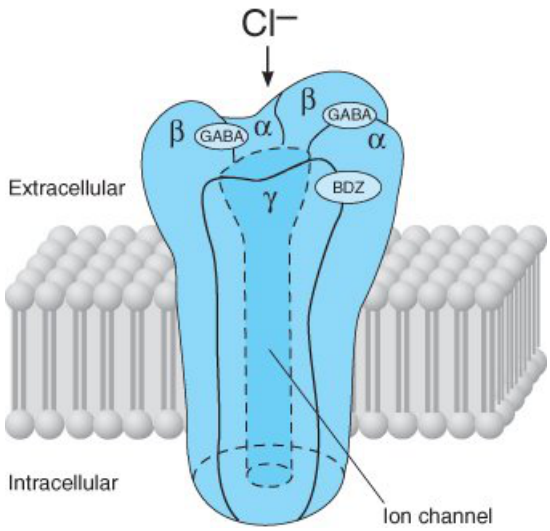

Figura 3.11: Schematic representation of GABA$_A$ receptor.

The effect caused with the anaesthetic drugs is concentration-dependent, with low concentrations submaximal GABA-induced currents are potentiated, with higher concentration the ion channel opens in the absence of GABA. Finally, with even higher concentrations of the anaesthetic drug, the flow of ions is inhibit leading to a neuronal hyperpolarization . The binding site with GABA$_A$ receptor is in an amino acid residue of the β_2 subunit[3].

There are also some anaesthetic drugs that interact with neuronal glycine and nicotinic acetylcholine receptors, which also control ionic channels, and mediate the response to noxious stimulus. The only anaesthetics that do not interact with GABA nor glycine receptors are the ketamine, nitrous oxide, cyclopropane and Xenon. These drugs inhibit a different ionic channels controlled by glutamate that are selective to calcium ions and are involved in the modulation of the synaptic responses, the drugs interact with the receptor N-methyl D-aspartate (NMDA).

In conclusion, the evidences support the conception that the major part of the IV anaesthetic drugs act through the GABA$_A$ receptors and some interactions with other ligand controlled ionic channels. In a different way, the inhaled act in a wide variety of molecular targets. Finally the nitrous oxide, ketamine and the Xenon induce the depression of the nervous system with the inhibition of the NMDA receptors and the activation of potassium channels.

In this work the anaesthetic drugs used were isoflurane, inhaled anaesthetic drug, and propofol, IV anaesthetic drug, and so in the next two sections these two drugs are presented.

3.3.1 Isoflurane

The isoflurane is an inhaled anaesthetic drug and, as the rest of the inhaled anaesthetics, its distribution in the organism follows the gradient of its partial pressure in the different tissues. In the lungs, the gases pass to the blood stream that takes the anaesthetic to the tissues, the intake of the anaesthetic end at equilibrium. When the partial pressure of the exhaled air is equal to the inhaled air the equilibrium is reached and the pressure of the anaesthetic drug is equal in every organ. At equilibrium, the DoA is kept if the administered pressure is maintained constant.

Isoflurane is the common name of 2-chloro-2-(difluoromethoxy)-1,1,1-trifluoro-ethane and it is a non-explosive volatile fluid at room temperature. As the rest of the inhaled anaesthetics, isoflurane has a small security band and this makes it one of the most dangerous drugs with clinical uses and so the use of this anaesthetic is carefully done with consideration of the patient's profile and his tolerance to its side effects.

The main side effects of isoflurane are hypotension that is counteract with the raising of the heart rate, the depression of the respiratory system and muscle relaxation. The majority of the anaesthetic is expelled through breath when the administration is stopped and the patient breaths freely.

3.3.2 Propofol

Propofol is the most used parenteral anaesthetic. The parenteral anaesthetics are small hydrophobic molecules that induce anaesthesia when an high dose is administrated, a bolus. The drug spreads to the most vascularized tissues, mainly to the brain and the spinal cord and the concentration in circulation decreases rapidly. Soon the anaesthetic is back in circulation and it diffuses to the less perfused tissues, like muscle and bowels where it lasts longer, and so the depression of the consciousness ends, not because of metabolism but due to the redistribution of the drug through all the body.

Its systematic name is 2,6-diisopropilfenol and it is a short-acting drug intravenously administered that induces hypnoses in approximately 40 seconds with minimal arouse. The initial bolus is between 1,5 and 2,5 mg/kg and a steady state may be found with rates of 0.1 to $0.3mg.kg^{-1}.min^{-1}$. Its half-life period is about 3 minutes and since it is not analgesic and so it must be used with some opioids to ease the pain.

It has some side effects in the blood pressure with the induction of vasodilatation and the depression of the contractibility of myocardium that lead to hypotension. The patients undergoing a anaesthesia induced with propofol must have the oxygen saturation monitored to ensure that the

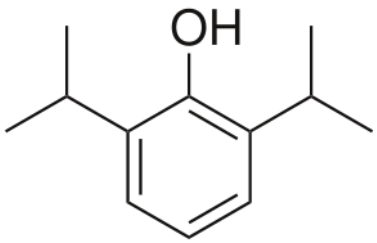

Figura 3.12: 2D structure of propofol.

ventilation is accomplished effectively.

3.4 Assessment of the Depth of Anaesthesia

Nowadays the assessment of DoA is accomplished through clinical analysis, the variations in the EEG signal and, in a anaesthesia induced with inhaled anaesthetics, the partial pressure of the drug in the exhaled air.

The anaesthetist look for evidences of the DoA in clinical signs like blood pressure, heart rate, sweat and lacrimation. To assess the state of consciousness he also inflicts some painful stimulation to the patient and his reaction or its absence helps the anaesthetist to predict the DoA. Since these signs do not depend only on the level of awareness and in order to control the evolution of the procedure other vital signals should be monitored, like oxygen saturation to control if the patient's ventilation is effective, the body temperature, exhaled gases, urine output to check the circulatory function, neuromuscular function and cerebral activity.

In 1847, John Snow and Francis Plomley tried to describe a set of procedures to assess the DoA, but it was just in 1937 that Arthur E. Guedel described the first detailed and widely accepted system. This classification system depended essentially upon the muscular movements and was designed for anaesthesia induced by ether. However, with the introduction of neuromuscular blocking agents and the use of other anaesthetics turned the Guedel's classification obsolete. Other scales were defined such as the RSS, Richmond Agitation Sedation Scale (RASS), Motor Activity Assessment Scale (MAAS) or the modified OAAS.

The RSS was the first scale used to classify the level of arousal of a sedated patient. It identifies the different stages of anaesthesia according to the responsiveness to verbal commands and reaction to painful stimulation. The table 3.1 presents the six different stages and the behavior presented by the patient.

It is an intuitively obvious scale and therefore lends itself to universal use, not only in the ICU,

Tabela 3.1: Ramsey Sedation Scale

Level of awareness	Presented Signs
1	Patient is anxious and agitated or restless, or both
2	Patient is cooperative, oriented and tranquil
3	Patient responds to commands only
4	Patient exhibits brisk response to light glabellar tap or loud auditory stimulus
5	Patient exhibits a sluggish response to light glabellar tap or loud auditory stimulus
6	Developing cognitive Patient exhibits no response

but wherever sedative drugs or narcotics are given. It can be added to the pain score and be considered the sixth vital sign.

As said before, the concentration of inhaled anaesthetics drugs is the same across all the different tissue when the equilibrium is reached, and so the DoA may be predicted based on the concentration of the exhaled air because the correlation between them has been studied and reported. The Minimal Alveolar Concentration (MAC) is a measure of the effectiveness of the anaesthetic drug that indicates the minimal concentration needed to block all responsive movements to the surgery's stimulation of 50% of the patients. There are some other reported values like the MAC$_{wake}$ that is the minimal concentration value for which half of the patients are still awake.

The analysis of the exhaled air is a simple process that uses mass's spectrophotometry and it gives the partial pressure of the anaesthetic drug in the alveoli that indicates accurately its partial pressure in the tissues in real-time.

In animal surgery, the control of the anaesthesia is still achieved through the analysis of some clinical signs such as cardiorespiratory parameters and also autonomic reflexes such as eye lid reflexes and responses to painful stimuli: tail, ear or paw pinch reflex. Thus, the control is not continuous and it is subjective which leads to a higher risk of death by overdose of anaesthetic [12].

Yet with the development of new techniques like the EEG and EMG some quantitative monitors emerge, such as Bispectral index (BIS), Auditory Evoked Potentials (AEP), the Patient State Index (PSI) and Narcotrend Monitor, that will to be more objective [30].

The fundamentals of the analysis of the EEG used to predict the DoA are presented in the next

chapter, chapter 4.

Chapter 4

Electroencephalography

In this chapter it is done a brief introduction of the EEG to present its history, the methods for acquisition of an EEGram and its utility in medicine.

The EEG is a technique to record the cerebral electric activity. This activity is generated by the communication between neurons within the brain. The potentials produced have to pass through the four different protective layers, pia mater, arachnoid mater, dura mater and skull. The activity registered in an EEGram is the result of the combination of thousands of neurons communicating with each other, firing action potential in their communicant cells.

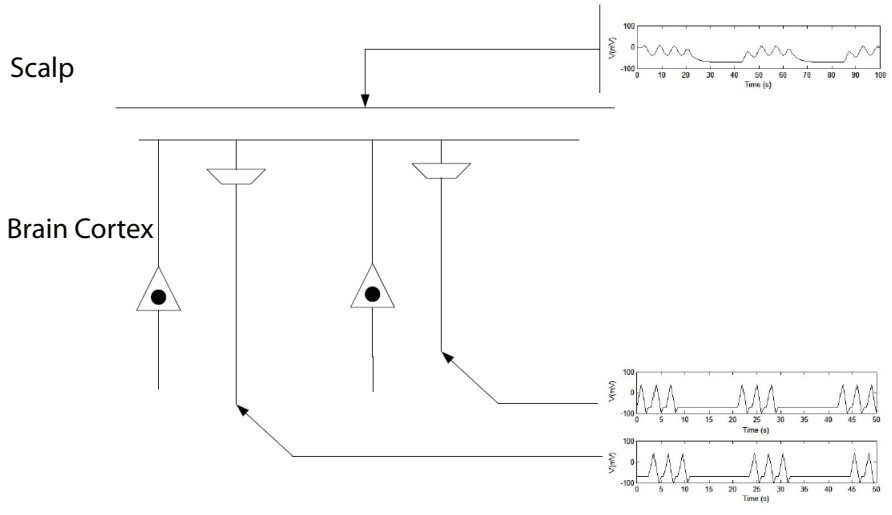

Figura 4.13: Representation of the nervous tissue and the electrical conduction of the signal. The triangular cells represent the glia cells while the other represent the neuron. The signal observed at the surface of the scalp is a combination of the both individual signal with some dissipation of its power.

Richard Caton was the first physician to explore the electrical activity of the brain. He presented

the trials performed in rabbits, cats and monkeys in [4] [5]. The first human EEGram was recorded in 1929 by Hans Berger.

In the last 50 years, the electroencephalographers changed the paradigm of the EEG. At the beginning, the scientists look for the tracing and its patterns, nowadays, the goal is to develop automatic analyzer systems. This evolution would led to a new world where EEG was fully computerized with automatic interpretation, so the electroencephalographers feared that they would be dispensable. However, this fear was unfounded because EEG is far too complex to such automation, and EEG is still fundamental in the diagnosis and for monitoring patients, neurologists use this exam to study and identify pathologies like epilepsy and sleeping disorders, anaesthetists for the monitoring of the DoA and scientists to deepen the knowledge of the brain functioning.

4.1 Electroencephalogram Acquisition

The regular EEG is a simple, noninvasive and painless method that uses a set of electrodes that are placed in the scalp after the area is abraded and a conductive gel is applied. In order to get some anatomical information, two dozen of electrodes are used in a standard configuration according to the International 10-20 system [33], as shown in figure 4.14.

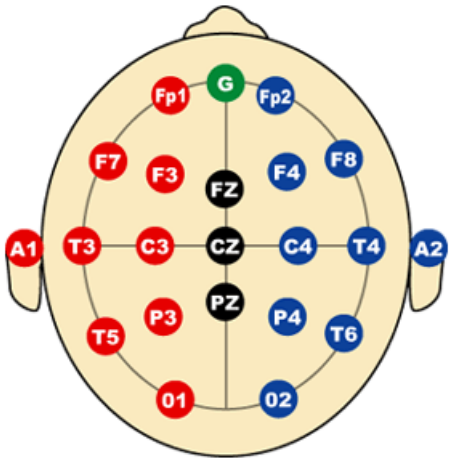

Figura 4.14: Schematic representation of the electrode placement in human electroencephalography. The even numbers are placed in the right hemisphere while the odd numbers in the left. This type of the distribution of the electrodes allow to study the anatomical activity of the brain.

The electrical potentials may be measured using different kinds of settings from which the most used is the bipolar setting, where the electrodes are paired and the amplitude is calculated as the voltage observed between the two electrodes. These electrodes are connected to differential amplifiers wherefore the signal is amplified. In analog systems the signal is then filtered and the output is written with deflection pens while paper passed underneath them. Nowadays most

of the EEGram are digital and the amplified signal is then converted with a analog-to-digital converter. The signal is still corrupted with different sources of noise. To remove artifacts of movement and electro-galvanic signals it is used a high-pass filter with cut-off frequency below 1 Hz, whereas to withdraw high frequency artifacts like EMG a low-pass filter set to $35-70$ Hz might be used. Finally the electrical power noise is cleared with a notch filter if the cut of frequency of the low-pass filter was higher than the fundamental harmonica of the electrical line. The typical sampling rates are between 256 Hz to 512 Hz and the normal recorded amplitude in the scalp by a EEGram lies between $10\mu V$ to $100\mu V$.

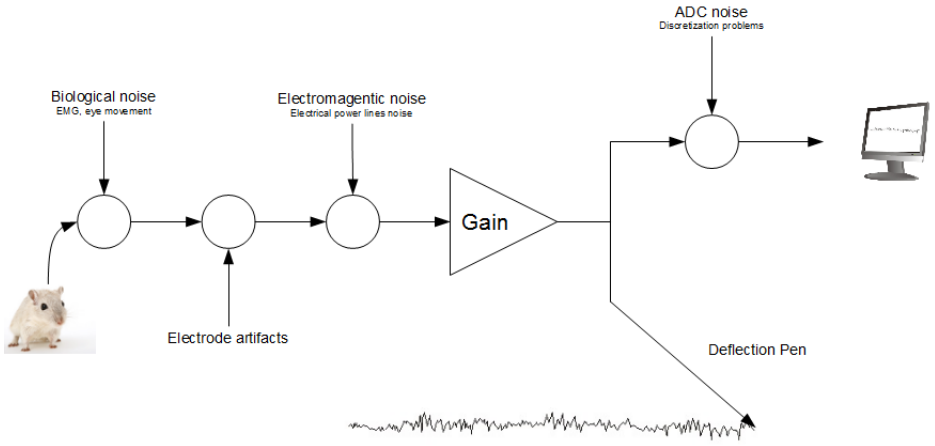

Figura 4.15: Schematic representation of the sources of noise along the EEG acquisition. The EEG signal is corrupted with biological noise from the muscular activity, eye movement, with electrode artifacts like variations of the skin impedance, with electromagnetic noise brought from the electric power lines, and in the digital EEGram there are also some noise from the discretization while converting analog to digital signal.

In some invasive techniques that want to reduce the noise enforced by the EMG, or to analyze some specific regions of the brain, the electrodes are be implanted directly into the target site so the amplitude recorded is higher in order of $500\mu V$ to $1500\mu V$. These techniques are called intracranial EEG and it was used in the data acquisition of a rat anaesthesia that is presented ahead in this dissertation.

4.2 Brain Waves

The spectrum of an EEGram is characterized by different frequencies from almost DC, $0.3Hz$, to $70Hz$ [22]. There are some bandwidths associated to some typical states of consciousness, the slower waves are the δ waves whose bandwidth extends to $3.5Hz$, these waves are typical of infants, adults sleeping and some tasks that require continuous attention. The θ waves are present during meditation, drowsiness or arousals and in young children too. The classical frequencies

of θ waves lays in the frequency range of $4Hz$ to $7.5Hz$. In a relaxed state the characteristic waves are the α waves, which have frequencies between $8Hz$ and $13Hz$. On the other hand, under stress, anxiety or alertness, the bandwidth of the electrical activity of the brain is from 14 to 30 Hz that represents the β waves. Finally, while developing cognitive functions or motor functions the EEGram exhibits frequencies higher than 30 Hz, these are the γ waves. The table 4.2 summarizes the different bandwidths and the states where each band is dominant.

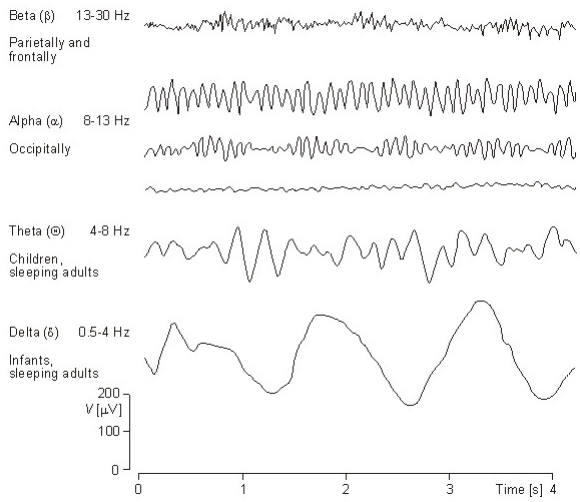

Figura 4.16: Representation of the typical EEG waves [20].

Tabela 4.2: Typical distribution of brain waves in different states of consciousness.

Brain Waves		
Wave	Frequency Range	Present in
δ	$[0.5-4]$	Adult slow wave sleep, babies
θ	$[4-8]$	Young children, drowsy or aroused adult, meditating
α	$[8-13]$	Relaxed with eyes closed
β	$[13-30]$	Alert or anxious adult
γ	$[30-60]$	Developing cognitive and motor functions

The α rhythm is a classical EEG sign for the state of relaxed wakefulness, these waves are blocked by emotional tensions, waves with the same behavior are observable in animals however the rhythm may be different, in the primates the α waves have frequencies above $10Hz$, while in cats between $8Hz$ and $13Hz$ or in young dogs it is found from $6Hz$ to $8Hz$ [22]. Although animals are used in many experiments the knowledged of its EEG patterns and the state of awareness is

still to explore so the analysis done in this thesis is based on the principles of the human EEG, the link between the human EEG and the veterinary medicine should be strengthened.

4.3 Analyzing the EEG

The analysis of an EEGram requires a well trained eye that is capable to recognize the distinct patterns that may be normal or abnormal which may be distinct due to variations in amplitude, frequency or both and so with an experienced eye is relatively simply to identify these changes, although it is quite difficult to translate this analysis to mathematical expressions. The identification of abnormal patterns is fundamental for diagnosis of diseases like epilepsy and it can be very useful in the control of the DoA.

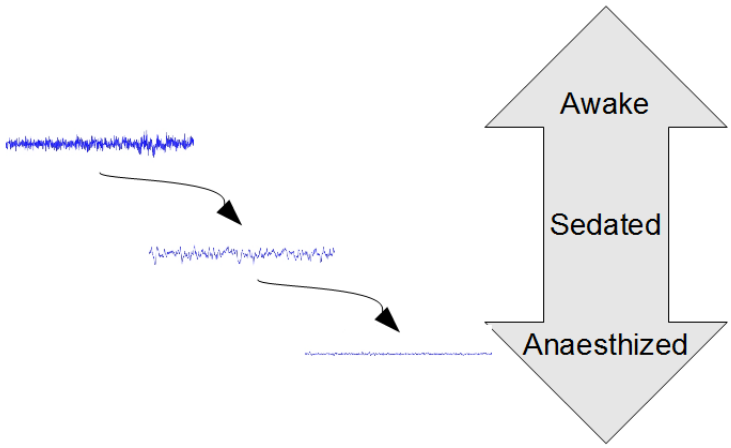

Figura 4.17: This is an illustration of the observable differences in the EEGram while the anaesthesia is induced.

During the induction of anaesthesia, with the beginning of anaesthesia in the intermediate states, the EEG signal commutes from a low-amplitude, large-bandwidth, noise-like signal to an high-amplitude and slow waves signal. In deeper level of anaesthesia, the EEG signal shows periods of burst suppression alternating with brain activity, the proportion of time with burst suppression may be used to characterize this anaesthesia state. In the deepest level of anaesthesia the signal resembles an isoelectric signal, i. e., there is no cortical activity [20]. The EEG of animals evolves in a similar way between the different stages of anaesthesia. These changes in the spectrum of the EEGram during anaesthesia may be related to the distribution of the power spectrum among each typical brain wave. Thus, as it is described in [22], while inducing anaesthesia the β waves start to present more activity, then with the deepening of the DoA the α waves vanish. In a deeper level very low amplitude of fast rhythms alternates with burst of high amplitude, when these bursts are absent and the signal is almost isoelectric a toxic level has been reached. The

Tabela 4.3: Typical brain waves in different levels of anaesthesia.[22]

Depth of Anaesthesia		
Clinical State	EEG features	Level
Awake	α Dominant	I
Excited	β Activation θ Induction	II
Early Anaesthesia	α - θ Dominant Some δ	III-1
Surgical Tolerance	δ Waves Dominant Some θ	III-2
Deep Anaesthesia	High Amplitude δ Waves	III-3
Early Overdose	Burst-Supression	III-4
Toxicity	Isoelectric	IV

table 4.3 summarizes this description.

Based on these variations some different approaches on the automation of the control of anaesthesia may be considered. On the one hand, a database with different signals from the well defined states is used to compare with a new unknown data. The reliability of this method depends on the database and its sources of error.

On the other hand, there are methods that calculate the DoA based on concepts of Entropy, SEF or bandwidth distribution and then analyze them with the theoretical knowledge. In the next chapter the different approaches will be considered and described.

Chapter 5

Analyzed Methods

This chapter presents the different methods used to predict the DoA based on the analysis of the EEG signal. These methods may be seen as mapping functions where the input is a feature of the acquired signal and the output is an index value that correlates with the DoA. In this thesis seven different methods were tested and two of those methods were also used with a correction factor, the BSR.

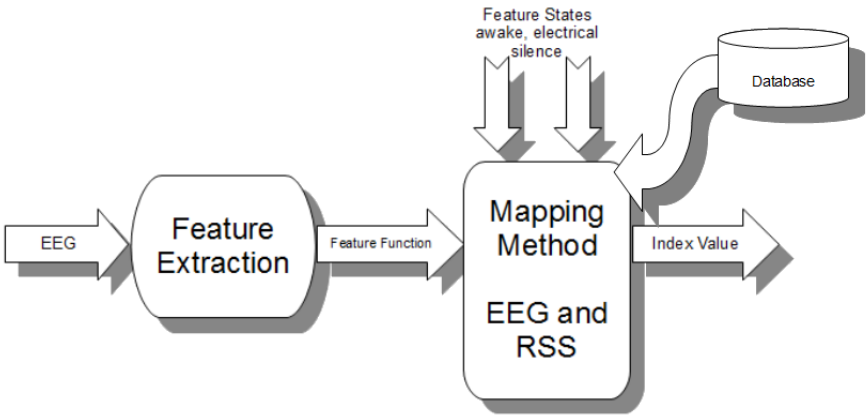

Figura 5.18: Schematic representation of a monitor index. This figure represents the generic method of predicting DoA based in the EEG signal

After the removal of the noise from the EEG with different sets of filters, some features of the signal are extracted and then mapped with some methods that interpolate the features to an index value correlated with the DoA. These methods may or may not use a database to analyze the features to predict the DoA based on previous experiments.

htb

Tabela 5.4: Presentation of the different analyzed methods

Name	Feature	Mapping Method
Permutation Entropy	Motif Distribution	Entropy
Shannon Entropy	Histogram	Entropy
Approximate Entropy	Pattern Repetition	Entropy
Spectral Edge Frequency	Power Spectrum	Integral function
Band Distribution	Power of the Brain waves	Imposed Condition
Two Limit State	Histogram or Power Spectrum	Norm
Finding Similar State	Histogram or Power Spectrum	Norm

5.1 Methods

In this section, the mathematical representation of each method is presented. The first method described is the PE [24], which calculates the entropy of the signal based on set of motifs and its distribution. Then another method to calculate the entropy is ShEn [9]. In that calculation the entropy is based on the Probability Density Function (PDF) of the signal. To conclude the methods based on the entropy of the signal the ApEn is a method that analyzes the repetition of patterns in the EEG.

After this, a method identifies the frequency below which lays 95% of the power of the signal, the method is called SEF. Then, the new approach based on the typical power distribution among the common brain waves of each different state is introduced.

Finally, the presentation of two methods, TLS and FSS, that resort to a database to identify different stages, is done.

The methods corrected with the BSR are the PE and the $\text{SEF}_{95\%}$.

5.1.1 Permutation Entropy

The PE uses as feature the distribution of the motifs created by consecutive points, with two points, two motifs can be generated as shown in figure 5.19, with three points, six different motifs, figure 5.20. The number of motifs generated by n_{points} follows the function 5.2.

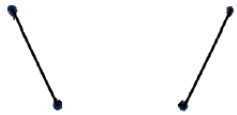

Figura 5.19: Schematic of the motifs used to catalog the EEG changes in time domain.

Figura 5.20: Schematic of the motifs used to catalog the EEG changes in time domain.

$$N_{PEmotifs} = n_{points}! \tag{5.2}$$

The method calculates the entropy of the distribution of the signal among these motifs. The shape of motifs is more complex with the growth of the number of points used, however a higher complexity do not provide better results [24]. In this work the number of points used was three points as suggested in literature [24].

The entropy is calculated based on the computation of the probability of the occurrence of the motifs which is given by the equation 5.5,

$$H_{PE} = \frac{\sum_{i=1}^{N_{PEmotifs}} p_{iPE} \times \log(p_{iPE})}{\log N_{PEmotifs}}, \tag{5.3}$$

where $N_{PEmotifs}$ is the number of motifs, and p_{iPE} is the probability of the i motif. The mathematical representation of the motifs with three points is represented in equation 5.4.

$$motifs = \begin{cases} x_1 < x_2 \wedge x_1 > x_3 \\ x_1 > x_2 > x_3 \\ x_1 > x_2 \wedge x_1 > x_3 \wedge x_2 < x_3 \\ x_1 > x_2 \wedge x_1 < x_3 \\ x_1 < x_2 < x_3 \\ x_1 < x_2 \wedge x_1 < x_3 \wedge x_2 > x_3 \end{cases} \tag{5.4}$$

In order to tolerate the interference of the noise, a threshold value is used and a different motif is considered when all the points have approximately the same value, $|x_1 - x_2| < \delta_{PE}$ and $|x_1 - x_3| < \delta_{PE}$.

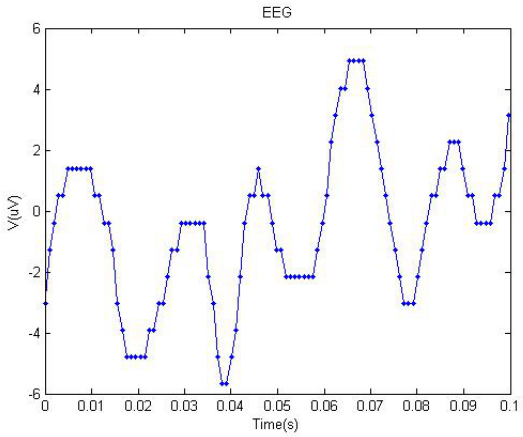

Figura 5.21: The discrete EEG acquire a finite number of points to register the brain activity. The relation between points may be analyzed and find different types of motifs according to the number of motifs used.

The value of δ_{PE} used for the rabbit experiment was 0.015 while for the rat experiment $0.2 \times std(EEG_{rat})$. The identification of the motif in the EEG is presented in figure 5.21.

5.1.2 Shannon Entropy

Also based on the same mapping method, the ShEn algorithm analyzes the entropy of the distribution of the amplitude of the signal.

When a signal is measured the PDF is unknown and to analyze the amplitude distribution, the PDF must be estimated. A good approximation of the PDF is the histogram. In this work were used k_{bins} bins, where $\frac{k_{bins}}{N_{ShEnpoints}}$ is a constant and $N_{ShEnpoints}$ is the number of points analyzed. The chosen ratio was 0.02, based on results found in literature [9]. The entropy value is then calculated according to equation 5.5,

$$H_{ShEn} = \frac{-\sum_{i=1}^{k_{bins}} p_{ShEni} \times \log(p_{ShEni})}{\log k_{bins}}, \tag{5.5}$$

where p_{ShEni} is the probability of randomly picking a point from the EEG with the amplitude in the interval i.

5.1.3 Approximated Entropy

Then ApEn is a method which analyzes the probability of the repetition of patterns in the observation of the signal. A predictable signal shows repetitive patterns and the ApEn index will be a

low value, on the other hand a noise like signal, very unpredictable will have a higher value of ApEn.

The first description of ApEn was done in [15] as an application to heart rate monitoring. In this approach the goal is to find matching patterns according to two defined arguments, m the specific length of each pattern and r the similarity criteria. A pattern is considered similar to other when equation 5.6 is verified.

$$|sn(i+k) - sn(j+k)| < r \; for \; 0 \leq k < m \tag{5.6}$$

Then a set of all patterns that can be created with length m from S_n, $P_m = [p_m(1), ...p_m(N_{ApEnpoints} - m+1)]$. From this set, the probability of finding a similar pattern to pattern $p_m(i)$ is calculated, $C_{im}(r)$,

$$C_{im}(r) = \frac{n_{im}(r)}{N_{ApEnpoints} - m + 1} \tag{5.7}$$

where n_{im} is the number of similar patterns and $N_{ApEnpoints} - m + 1$ is the number of all patterns. Finally, ApEn value is calculated as,

$$ApEn(Sn, m, r) = ln[\frac{C_m(r)}{C_{m+1}(r)}] \tag{5.8}$$

where $C_m(r)$ is the mean value of $C_{im}(r)$ for $i = 1, 2...N_{ApEnpoints} - m + 1$. In the work developed in this thesis, the length of the patterns were of 2 points and the similarity criteria value of 0.2 as it was used in [28].

5.1.4 Spectral Edge Frequency

The SEF_{95} identifies the frequency below which is located 95% of the power of the signal.

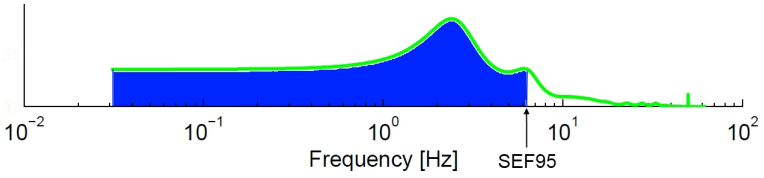

Figura 5.22: The blue area represents 95% of the power of the signal and at its edge the SEF95.

This method uses as feature the power spectral distribution calculated with the aid of the Fast Fourier Transform (*fft*) function of MatLab and identifies the shift in frequencies experienced with

the deepening of the level of anaesthesia. The input of the algorithm is the EEG signal and identification of the intent frequency is accomplished with a simple method of search.

5.1.4.1 Fourier Analysis

The concept of Fourier Analysis is that every general function may be represented by a sum of different trigonometric functions. A trigonometric function, sine or cosine, have a characteristic frequency and so the frequency distribution of a function is calculated with the Fourier Transform.

$$F(\nu) = \int_{-\infty}^{+\infty} f(t).e^{-2\pi i\nu t}dt \tag{5.9}$$

To transform a time domain discrete function into a frequency domain function is used the Discrete Fourier Transform, that is the representation of the initial function in the frequency domain.

$$X_k = \sum_{n=0}^{N-1} x_n e^{-\frac{2\pi i}{N}kn} \quad k = 0, ..., N-1 \tag{5.10}$$

$$x_n = \frac{1}{N}\sum_{n=0}^{N-1} X_k e^{\frac{2\pi i}{N}kn} \tag{5.11}$$

The efficient method to compute the Discrete Fourier Transform is the Fast Fourier Transform, which is the algorithm used to compute spectral distribution in this algorithm.

The Burg method is an autoregressive method to extract the power spectral density from the result of an Fast Fourier Transform, and this method was used in the elaboration of the database of the frequency analysis.

5.1.5 SEF and PE corrected for burst suppression ratio

In the deepest levels of anaesthesia, the EEGram develops patterns, known as burst suppression, characterized by periods of regular or high voltage activity turning to low voltage, almost isoelectric pretending that there is no brain activity. The BSR may be used in the control of anaesthesia and to calculate this parameter, a period of suppression is identified as "those periods longer than 0.50 s, during which the EEG voltage does not exceed approximately ± 50 mV."[26]. The length of the suppressed time is accounted and the BSR is the respective fraction of the epoch in analysis.

The index calculated with PE and SEF is then corrected with the value of BSR as shown in 5.12.

$$Index_{corrected_BS} = Index(1 - BSR) \tag{5.12}$$

This correction proves to be very useful in the identification of deep levels of anaesthesia.

5.1.6 Band Distribution

This new approach was called BD method. The method analyzes the power distribution among the typical bands presented in table 4.2 and tries to identify the patterns of each state of anaesthesia presented in table 4.3. In this way, the algorithm begins with an analysis on the amplitude of the signal to infer if the data acquire is typical from a deep anaesthetized subject. If this condition is false then the signal is separated with a block of pass-band filters with the limits set for the EEG brain waves, see figure 5.23. Then the instant power signal is calculated and finally the energy of it.

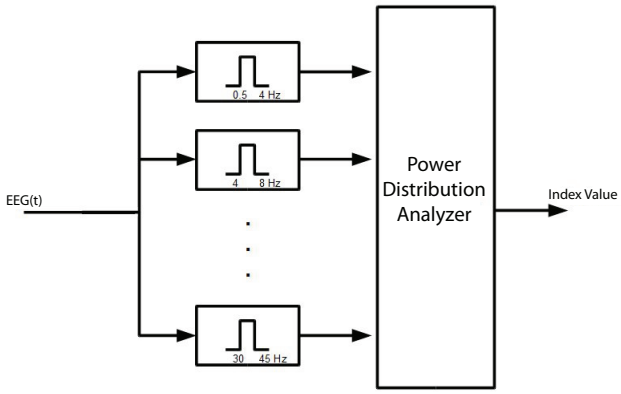

Figura 5.23: The signal is separated with this block of filters with no gain. The pass-band filters have its limits set to identify the typical brain waves.

After this, an analysis of the band distribution identifies the different states in a discrete way. If the band with major representability is the α wave then the subject must be awake, on the other hand, if β wave significance is higher than a third of the all signal then a state of excitement is experienced. But if the sum of α waves and the θ corresponds to 80% of the signal it is assumed a state of light anaesthesia, when the δ has the higher concentration of power it is considered the deep anaesthesia state, and finally the surgical tolerance level is assumed when the sum of δ and θ makes up 80% of the total power. In order to produce a index bonded between 0 and 100 a number was attributed to each of these states. The awake state as a score of 100, then, assuming the excitement is the initial effect of the anaesthetic, 80, the value of light anaesthesia

Tabela 5.5: Conditions to identify a specific state of anaesthesia. [22]

Condition to Control		
Clinical State	EEG features	Level
Awake	α waves contains the highest power.	I
Excited	β Dominant Some θ	II
Early Anaesthesia	α - θ Dominant Some δ	III-1
Surgical Tolerance	δ Waves Dominant Some θ	III-2
Deep Anaesthesia	High Amplitude δ Waves	III-3
Early Overdose	Burst-Supression	III-4
Toxicity	Isoelectric	IV

is 60, 40 corresponds to the surgical tolerance, 20 to the deep anaesthesia and finally 0 to the almost isoelectric signal.

The identification of each state is discrete and to produce a continuous index the result was filtered with a mean filter, equation 5.13, accounting the late 30 predictions.

$$index(i) = \frac{1}{N_{window}} Level_{predicted} + (1 - \frac{1}{N_{window}}) index(i-1) \tag{5.13}$$

The filtering is processed simultaneously as the DoA identification. The implementation of this algorithm is presenting in the Appendix B

5.1.7 Two Limit States

The TLS method is a method that resort to a database to define a bijective function, $h(x)$, with two boundary state values, state *a* and state *b*, where $h(a) = 1$ and $h(x) = 0$, with a monotonically trend between them.

$$h : \mathbf{x} \in [a, b] \rightarrow i \in [0, 1] \tag{5.14}$$

These frontiers correspond to the awake and deeply anaesthetized states. This function does the comparison of the feature of the extreme states and the intermediate and unknown state. The feature may be a vector or a scalar, for instance, the power spectrum, the PDF, the mean value or anything that characterizes the section of the signal under analysis. In order to implement this

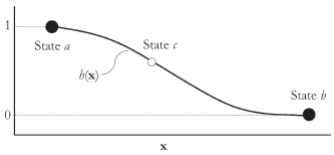

Figura 5.24: The function h is a bijective function. In this case it is assumed that the system evolves monotonically and so the function h as to be monotonic too.

method, a database of the two extreme states needs to be acquired,

$$\begin{cases} R_a = \mathbf{x}_{a,k}, & k = 1, 2, ...M \\ R_b = \mathbf{x}_{b,k}, & k = 1, 2, ...M \end{cases} \tag{5.15}$$

where $\mathbf{x}_{a,k}$ and $\mathbf{x}_{b,k}$ are vectors with a finite number samples, belonging to the k^th epoch of the data sets R_a and R_b. Then, the selected feature, $f(\mathbf{x}) = \mathbf{f}$, is extracted from each epoch and the mean value or vector calculated,

$$\begin{cases} \overline{\mathbf{f}_a} = \frac{1}{M} \cdot \sum_{k=1}^{M} \mathbf{f}_{a,k} \\ \overline{\mathbf{f}_b} = \frac{1}{M} \cdot \sum_{k=1}^{M} \mathbf{f}_{b,k} \end{cases} \tag{5.16}$$

used to compare with the unknown state. To predict an index value the vectorial distance between the intermediate state *c* and the reference states. This is accomplished with difference among the feature values of the states,

$$\begin{cases} j_\alpha = \|\mathbf{f}_c - \overline{\mathbf{f}_a}\|_1 \\ j_\beta = \|\mathbf{f}_c - \overline{\mathbf{f}_b}\|_1 \end{cases} \tag{5.17}$$

with $\mathbf{f}_c = f\mathbf{x_c}$ and the operator norm $\|\cdot\|_1$ is defined as

$$\|\mathbf{v}\|_1 = \sum_{n=1}^{N} |v(n)| \tag{5.18}$$

These two indexes may be combined to form a single value, $j = j_\beta - j_\alpha$. And now function $g(x)$ is determined,

$$g : \mathbf{x} \to g(\mathbf{x}) = j = \|f(\mathbf{x}) - \overline{\mathbf{f}_b}\|_1 - \|f(\mathbf{x}) - \overline{\mathbf{f}_a}\|_1 \tag{5.19}$$

In order to normalize the index *i* between $i \to 1$ (state a) and $i \to 0$ (state b),

$$h : \mathbf{x} \to h(\mathbf{x}) = i = g(\mathbf{x}) \cdot \frac{1}{\overline{j_a} - \overline{j_b}} - \frac{\overline{j_b}}{\overline{j_a} - \overline{j_b}} \tag{5.20}$$

where $\mathbf{j}_a$ and $\mathbf{j}_b$ are calculated by equation 5.21,

$$\begin{cases} g : R_a \rightarrow \mathbf{j}_a = \{j_{a,k}, \quad k = 1, 2, \ldots, M\} \\ g : R_b \rightarrow \mathbf{j}_b = \{j_{b,k}, \quad k = 1, 2, \ldots, M\} \end{cases} \tag{5.21}$$

Finally, the result is multiplied by 100 to return the index value in the same scale as most commercial monitors.

The features used were histogram and frequency distribution calculated with the aid of the MatLab function *pburg*.

5.1.8 Finding the Similar State

The last method is the FSS that identifies the DoA with the comparison of the power distribution of the EEG through the different brain waves and a reference set acquired, a database where each different level of DoA is characterized by the mean value of some well identified epochs. The different identified states are the same five states that are clinically observed and were described in table 4.3.

The similar state is identified as the one with the lowest vectorial distance, equation 5.22.

$$vect_{power} = |power_{dist} - database_i|; \tag{5.22}$$

The algorithm determines the nearest state identifying the DoA from this data. Like in the methods of the bandwidth distribution, each state has a correspondent value and in order to have a continuous index the result was filtered with the mean filter presented in equation 5.13.

5.2 Analysis of the Algorithms

In this section the implemented algorithms are analyzed in the concerning of the time consumption and the efficiency. Basically, the number of operations executed for each time the function is called are calculated. The time consumed with every operation, multiplication, addition or comparison was considered the same. The table 5.6 presents the approximate number of operations executed of each implemented algorithm.

The commercial monitors use different approaches, for instance BIS index® [2] combines frequency and time domain techniques, the IoC-View® [21] uses symbolic dynamics methods integrated with burst suppression and β ratio, which is the fraction of the power of the EEG that

Tabela 5.6: Run-time and time complexity analysis.

Method	Number of Operations
PE	$> 10^3$
ShEn	$> 10^3$
ApEn	$> 10^7$
SEF	$> 10^4$
BD	$> 10^4$
TLS	$> 10^3$
FSS	$> 10^4$

corresponds to the β waves. The Narcotrend index [17] is based on extraction of quantitative features from a database of EEG traces, in time and frequency domain, classifying into stages from A (awake state) to F (isoelectric signal).

In the next chapter, the experimental procedures to acquire the data from rats and rabbits are described.

Chapter 6

Experimental Procedures & Results

This chapter does an overview of the experimental procedure used to collect the EEG data, the processing of the signals and the presentation of the results obtain. Two different experiments were executed, one was done in a rat where were used implemented electrodes in the cortex of its brain and the anaesthesia was induced with isoflurane, the other procedure was done in five rabbits and the data was acquired with the commercial equipment of the monitor IoC-View®, the anaesthetic used was propofol. The goal of both experiments was to collect EEG data from different DoA.

Both experiments were conducted by Dra. Aura Silva and Dr. Luís Antunes, both veterinary doctor of the *Centro de Ciência Animal e Veterinária* of the *Universidade de Trás-os-Montes e Alto Douro*. All experiments were conducted accordingly to ethic lines for animal experimentation[1].

6.1 Rat Experiment

The subject used in this first experiment was a male Sprague-Dawley rat weighing around 400 grams, free from recognized respiratory pathogens. Before the experiment, the rat had free access to food and water, and it was kept in a 12 hours daily/night cycle, with a constant temperature of 21$\pm$2ºC and a relative humidity between 50% and 70%.

One week before performing the experiment, at the same hour, in the daily period of the rat, the animal was submitted to a craniotomy to implant two matrices with 4 microelectrodes each, in the cortex and thalamus of its brain. These electrodes were then linked to the IoC-View cable device. The craniotomy was closed with acrylic dental cement. After the procedure the rat was

[1] According to the European Community directive number 86/609/ECC from the 24th November of 1986

transferred to a recovery box where, for 3 days, it received every 24 hours 2.5-5 mg of carprofen, an analgesic, and 3 mg of amoxicillin, antibiotic.

After the recovery, the rat was put inside a anaesthetic chamber before the recording of the data, so that it could get used to the space, avoiding the stress during the experiment. The record of the data began while the animal was still awake. Then the induction was accomplished with a 4-5% of isoflurane. After the loss of righting reflex and the evaluation of respiratory rate changes, the rat was transferred to a maintenance chamber where the concentration of isoflurane commuted from 1.1%, 1.4% and 1.7%. The evolution of the anaesthetic concentration is presented in 6.26.

6.1.1 Data Acquisition

With the implanted matrix, 8 different channels were available, 4 of them dedicated to analyze the cortex and the other half the thalamus, sampled at 500Hz collecting 3.2×10^6 samples

The figure 6.25 shows an overall view of the experimental set-up and the EEG signal obtained from one channel of the cortex is presented in figure 6.26 together with the command of the isoflurane anaesthetic.

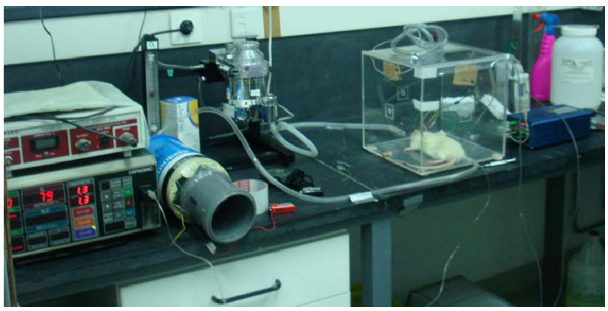

Figura 6.25: Experimental set-up

6.1.2 Algorithm Implementation

The data was filtered by low pass filtering with a butterworth filter of 8^{th} order and cut frequency at 40Hz. This value was appropriate to remove the 50Hz contamination and yet keeping the important frequencies to compute DoA indexes. After this, the mean value of the signal was removed in order to get out any threshold. Finally, to minimize the influence of factors such as electrode impedance and its placement, the data was normalized by the maximum value acquired in each channel. For processing purposes a decimation (factor 4) of the signal was performed.

In this experiment, the algorithms used a sliding window of 20 seconds with 2500 samples.

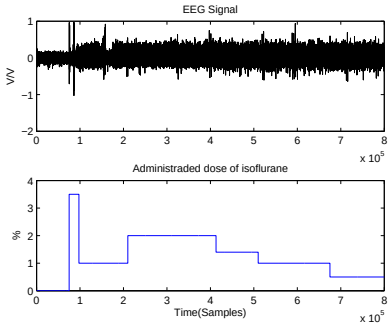

Figura 6.26: Graphics of the whole data acquired, the global evolution of the EEG signal and the dose of isoflurane given to the rat.

For the application of the comparative method with two reference states, the patterns of the EEG used to characterize the awake state were the following time intervals, first starting in the 1st, the second in 10th and 440th seconds, and to the anaesthetized state the periods start at 800th, 1200th and 3840th seconds. Figures 6.27, 6.28 and 6.29 presents three different states, the initial state, the deep anesthetized state with a deep burst suppression and intermediate anesthetized state with burst suppression.

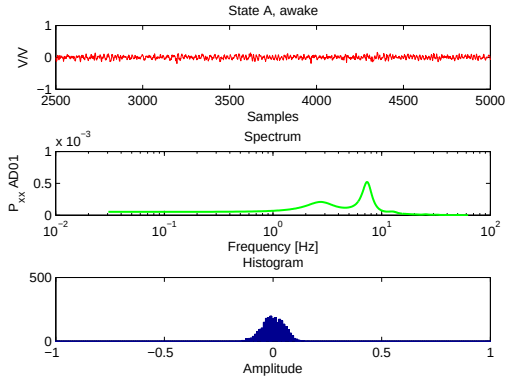

Figura 6.27: Initial state. Top - time segment window, middle - spectral density power, bottom - histogram of amplitudes.

In each figure a segment of the EEG signal is shown with the corresponding power spectral density, computed with the Burg method and the amplitude histogram. It can be seen that, from the initial state to the deep state, there is shift in the power density peak from high frequency to lower frequency and a narrowing in the amplitude histogram. This is in accordance with literature on the area [10][18].

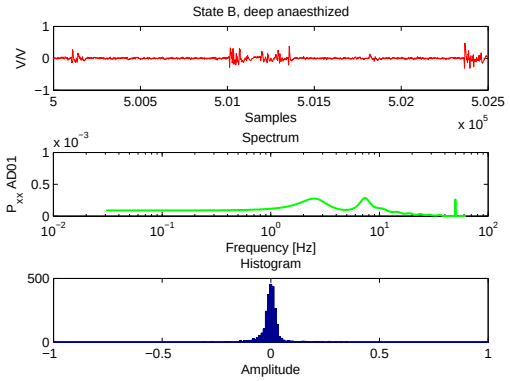

Figura 6.28: Deep anesthetized state based with a deep burst suppression.

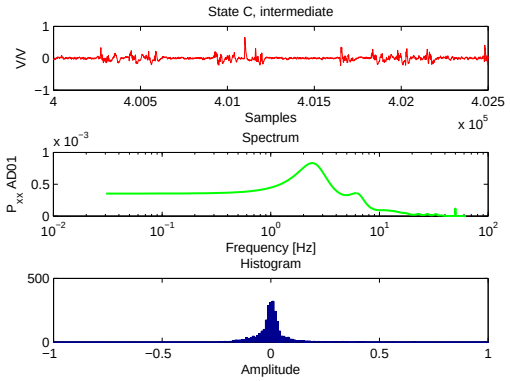

Figura 6.29: Intermediate anesthetized state with burst suppression.

6.1.3 Results

In figure 6.30 the variation of inflow of the anaesthetic used, isoflurane, is presented. The DoA should evolve along inversely to the concentration of the anaesthetic, and so the administered initial bolus get the rat into a very deep state of anaesthesia, then different steps were used to get different stages.

In figure 6.31, in green, the predicted index based on the distribution among the typical brain-waves. The index predicts that the rat was already anaesthetized in the beginning of the experiment, and it follows the changes in the anaesthetic drug given.

In figure 6.32, in purple and light blue the $\text{SEF}_{95\%}$ and the version corrected with the BSR are presented, respectively. The corrected version of the $\text{SEF}_{95\%}$ identifies deeper stages of anaesthesia correlated with the expected DoA due to the concentration of isoflurano. The $\text{SEF}_{95\%}$ show higher values to the deep states because the global power of the EEG signal decreases and so,

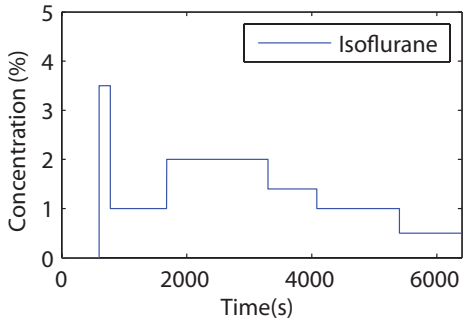

Figura 6.30: Representation of the variations of the concentration of isoflurane along time.

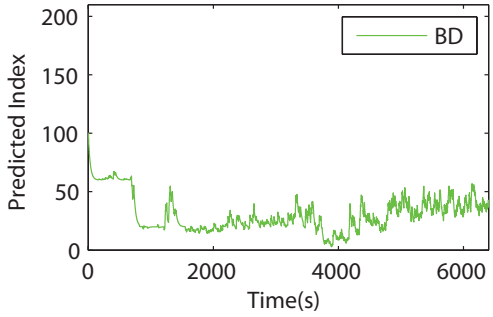

Figura 6.31: Plot of the index predicted with the BD method.

the power spectrum is spread through all the frequencies.

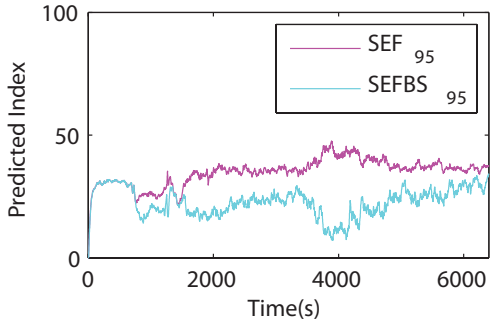

Figura 6.32: Presentation of the index predicted with the $SEF_{95\%}$ method in purple, and the SEFBS method in light blue.

The figure 6.33 presents in blue the ApEn index and in red the ShEn index, this indexes are constricted to a tight band of values and so they do not identify any different level of DoA.

The PE like the $SEF_{95\%}$ have a better performance when associated with the BSR, however it can be said that both of the indexes, PE and PEBS are correlated with the expected index, these methods are presented in figure 6.34.

The figure 6.35 shows in red the predicted index with the TLS method with the histogram as the

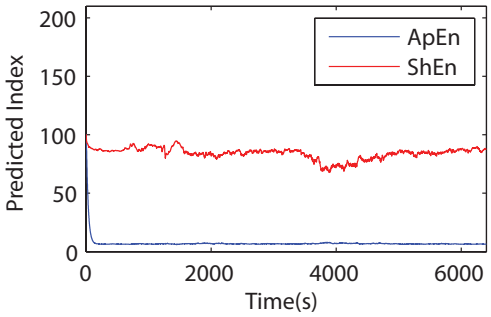

Figura 6.33: Presentation of the index predicted with the ApEn method in blue, and the ShEn method in red.

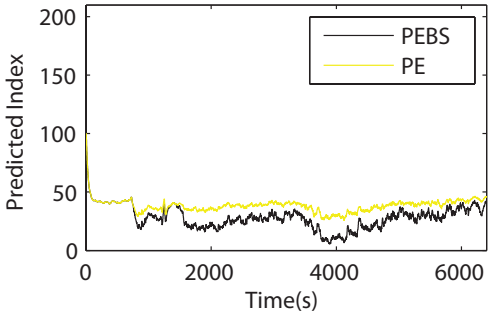

Figura 6.34: Presentation of the index predicted with the PE method in yellow, and the PEBS method in black.

feature. The index follows the variations in the anaesthetic drug given.

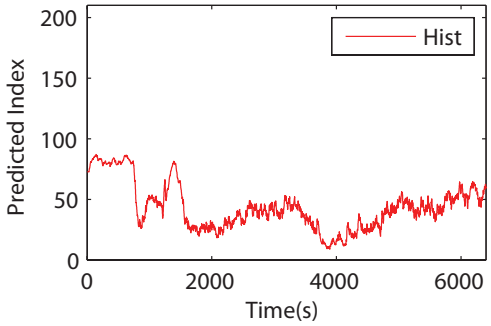

Figura 6.35: Presentation of the index predicted with TLS method using the histogram as feature.

In the last plot, presented in figure 6.36, illustrates in green the index obtained with the result of the application of the TLS method with the power spectrum as the feature. This method is a good approximation of the expected index too.

There are no results with the FSS method because in this experiment there was no information about the clinical assessment of the DoA and so it was impossible to elaborate a database with five different levels of anaesthesia. It must be emphasized that in recorded EEG data, there is a

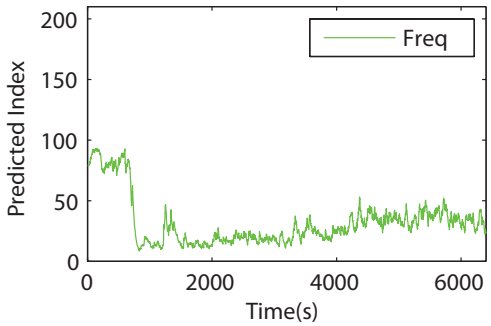

Figura 6.36: Presentation of the index predicted with TLS method using the power spectrum distribution as feature.

fast transition between the initial state to the state with burst suppression. There is no evidence of intermediate states between the initial state and the burst suppression. And so the methods must be evaluated with other EEG data with different levels.

6.2 Rabbit Experiment

The second experiment was preformed in five healthy rabbits. For the application of the electrodes the rabbits' heads were shaved and the skin was cleaned with a swab impregnated with acetone. The anaesthetic drug used was propofol and its infusion was controlled with an automatic syringe with adjustable speed of release of the fluid. The EEG signal was acquires with the IoC-View® monitor which has a complete set of electrodes. The experimental set up is presented in the figure 6.37.

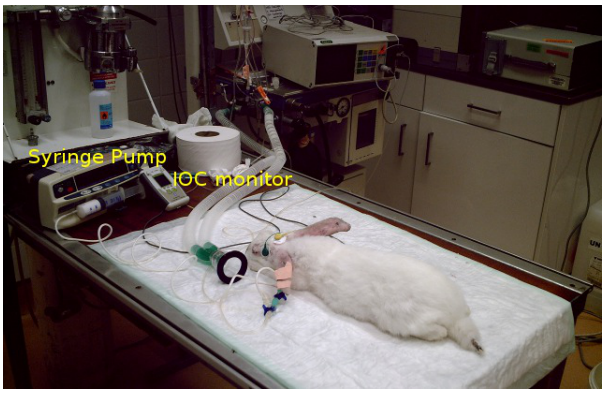

Figura 6.37: In the picture the experimental set up is presented. The rabbit was already anaesthetized.

6.2.1 IoC-View

The IoC-View® is a monitor of the level of consciousness for human anaesthesia that predicts DoA and registers the EEG signal. The EEGram is collected using three electrodes placed on the skin of the subject according to figure 6.40

Figura 6.38: The IoC-View®monitor is a little bit bigger than a common mobilephone. In the screen it plots the EEG and the predicted index.

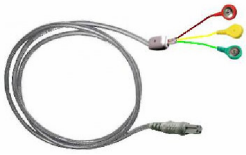

Figura 6.39: The IoC-View®monitor is connected to the patient with a cable with three leads.

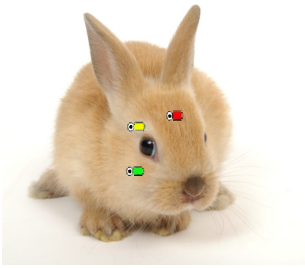

Figura 6.40: The electrodes are placed as illustrated in this picture, the red electrode in the center of the forehead, the yellow in the right side of the forehead and the green on in the cheek bone.

The predicted value of DoA with the IoC-View® limited between 100 and 0, where 100 corresponds to the awake state and 0 to the isoelectric signal. Sometimes, the IoC-View® may display higher values in the predicted index, these values are warning messages so that the user knows that there are some issues with the connections and the IoC-View® is preforming some tests to evaluate if everything is well placed.

In this experiment the IoC-View® was used as the data acquisition system to sample the EEG with a frequency of 1024 samples per second.

Tabela 6.7: Amount of anaesthetic drug administered.

Rabbit number	Sequence of infused propofol ($\frac{ml}{h}$)		
1 (initial time)	70 (1009 s)	130 (4996 s)	100 (5877 s)
2 (initial time)	100 (3019 s)	70 (1150 s)	130 (4954 s)
3 (initial time)	130 (3243 s)	70 (5382 s)	100 (1216 s)
4 (initial time)	100 (3720 s)	70 (1970 s)	130 (5926 s)
5 (initial time)	70 (800 s)	100 (2757 s)	130 (4563 s)

6.2.2 Procedure

The experiment consisted in the registration of the EEGram while the rate of administration of propofol was changed. To each rabbit a different sequence of rates of anaesthetic drug given, presented in table 6.7, were used. Each rate was maintained for half an hour and the depth of anaesthesia was measure every five minutes, twenty minutes after the change of the infusion rate.

6.2.3 Results

In this section, only the results obtained with the rabbit 5 are presented because this signal has less noise than the other signals from the rabbit experiments. Regardless of the noise present in the rest of the data, the results obtained with the other rabbits are very similar and are presented in the Appendix A.

In figure 6.41 shows the variation of the rate of the anaesthetic drug used, in this case propofol, to each set of steps induced different levels of DoA, as it is presented in the figure 6.42, clinical analysis. The identification of the DoA was accomplished with the common procedures of the RSS, this sets the expected evolution of the different indexes.

In figure 6.43 the the IoC-View® index is presented in red. This index does not identify the deepest level of DoA, which indicates that this index is unadapted to animal anaesthesia. In the same plot, in green, the BD index shows a close resemblance to the expected trend.

The $SEF_{95\%}$ and the version corrected with the BSR are presented in figure 6.44 in purple and light blue . Again, the corrected version of the $SEF_{95\%}$ identifies every stage of anaesthesia and it is a very good approximation of the clinical analysis and very close to the BD index. In this

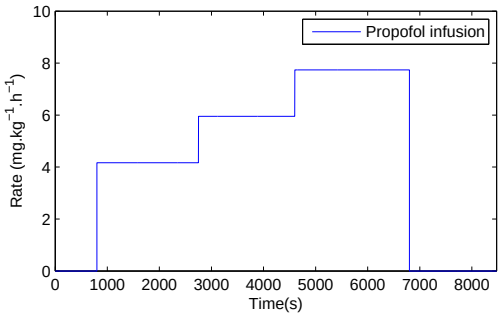

Figura 6.41: Representation of the variations in the rate flow of the propofol.

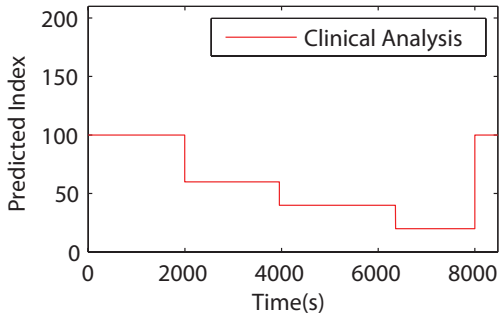

Figura 6.42: Empirical assessed of DoA.

experiment, the SEF$_{95\%}$ does not distinguish the deep states.

The figures 6.45 and 6.46, present the different methods based on the entropy value of the signal. In blue ApEn is presented, the red plot corresponds to the ShEn index, in yellow and in black are represented the PE and the PEBS, respectively. In this experiment the ShEn is ”able” to identify the deeper state of anaesthesia, however, the ApEn is still unable to distinguish any level of DoA.

As in the rat experiment, the PE like the SEF$_{95\%}$ have a better performance when associated with the BSR, however both of indexes, PE and PEBS are correlated with the expected index.

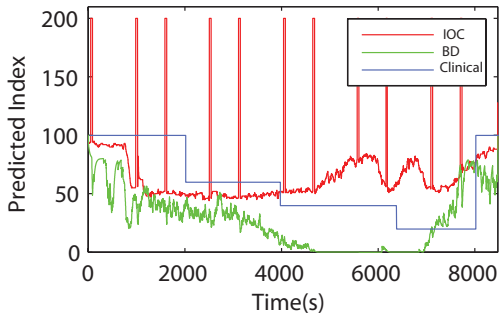

Figura 6.43: In this plot DoA predictions are the IoC-View® is presented in red and the BD index is in tones of green.

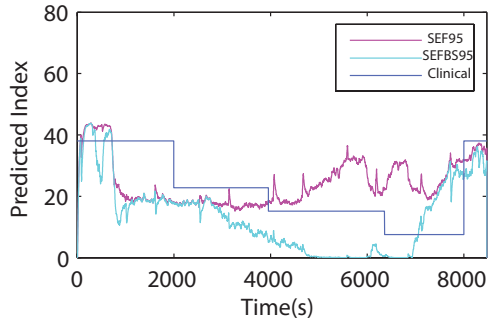

Figura 6.44: This plot represented the indexes calculated with the $SEF_{95\%}$ with and without the correction factor of the BSR.

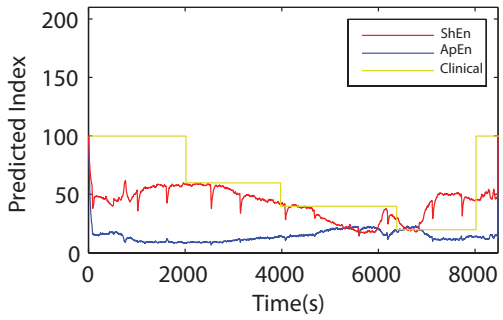

Figura 6.45: This plot represented the indexes calculated with the ApEn and ShEn methods.

The figure 6.47 presents the plot in green of the index calculated with the FSS method, and the IoC-View® index in red. As it is observable, these two indexes have similar shapes, however it is quite different from the expected index.

Finally the last plot, in figure 6.48 shows in black the predicted index with the TLS method with the histogram as the feature. This index predicts the deepest level of anaesthesia but is is unable to distinguish the shallower ones. Finally the index predicted with TLS method using the power spectrum as the feature is plotted in the same window in yellow. From the group of methods that

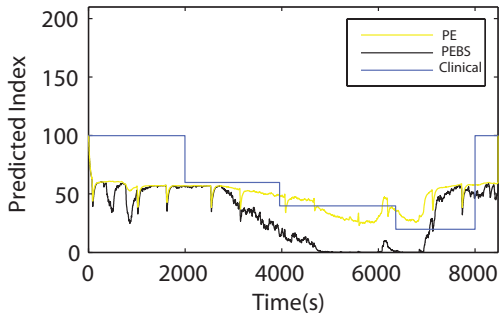

Figura 6.46: This plot represented the indexes calculated with the PE with and without the correction factor of the BSR.

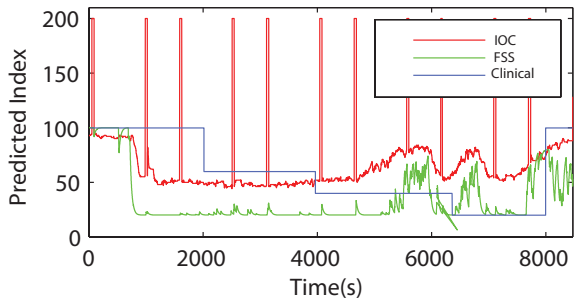

Figura 6.47: Plot with the index calculated with the IoC-View® and with the FSS method.

resort to a database, this is the best one, however it is not as accurate as BD index and SEFBS index.

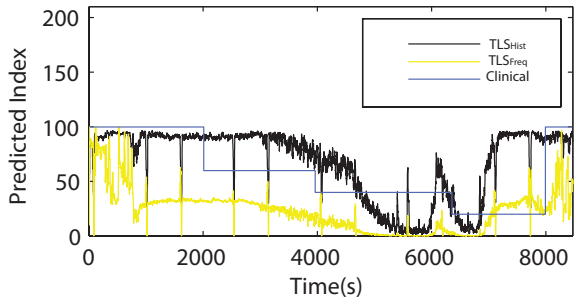

Figura 6.48: In this picture, the TLS method is presented using two different features, in black the histogram and in yellow the power spectral distribution.

Chapter 7

Conclusions

In this final chapter the main conclusions and contributions of the dissertation are summarized and the way for further work is pointed as well as aspects to improve the control of anaesthesia in animals.

7.1 Conclusions

The objective of this thesis was to analyze the performance of different algorithms in the prediction of the DoA in animal anaesthesia. The algorithms implemented and analyzed may be separate into two groups, the methods that resort to a database and the methods that are independent from databases. Although the database of each level was restricted and its affinity to the tested signals, the conclusion is that the results obtained with the TLS method with both features are similar to the ones achieved with the independent methods and so it is not worth to perform a set of experiments just to prepare the database to used in these methods. Moreover, the gains gathered from the reduction of the computational workload are insignificant.

The results presented in chapter 6 showed that the ApEn with the variables used is unable to identify any stage of anaesthesia, moreover it is a complex algorithm and the theoretical relation with DoA is unclear. On the other hand, the ShEn seems to identify the deeper states of anaesthesia but the index values for different shallow states of anaesthesia are almost identic. The best entropy method is the PE, although it is constricted in a tight gamut of index values, it identifies different stages and when corrected with the BSR it is a good approximation to the clinical analysis.

Although the $SEF_{95\%}$ is a good classifier for the light states but in deeper stages of anaesthesia it

gives unreliable index values due to the decrease of the global power of the brain waves and the growth of the influence of the noise scattered through all the frequencies. Again, the BSR is an extremely good method to correct this fault, the combination of $SEF_{95\%}$ with the BSR seems to be one of the best methods. Although the produce index is a frequency value it can be standardized to evolve from the value 100 which corresponds to the awake state to 0 the equivalent of the isoelectric state and in order to correlate with monitor indexes. Since the environment in the Operating Room (OR) is frightening which raises the anxiety levels of the patient and so the EEGram will be dominated by the β waves and the $SEF_{95\%}$ will register higher values. Then, the index can be normalized by multiplying a factor like $\frac{100}{Fc}$, where Fc is the cut off frequency of the low-pass filter used in the preprocessing of the signal.

The index produced with the band distribution analysis is similar to the identification of the DoA accomplished with the $SEFBS_{95\%}$ algorithm. In the rabbit experiments, in the profound stages of anaesthesia this method has a better performance than the IoC-View.

The methods that resort to a database due to the insufficient data provided for the elaboration of the database, seems to struggle in the classification of different stages of anaesthesia. However, based in these results it can be said that the best feature to use is the frequency distribution.

The number of tests executed were insufficient to validate the results obtained and some other indexes with proven efficiency should be used to compare these results.

In conclusion, to produce a good index it must be considered both frequency and amplitude characteristic. The SEF seem to be the best analyzer of the frequency features. However, the amplitude variations may be analyzed too and the correction with the BSR is the better option. The implemented method, the BD method, is a attempt to reply the SEFBS with the reduction of computational workload and some theoretical bases. These are the two best indexes from the group in analysis.

7.2 Future work

Hopefully, this thesis may contribute to the development of an autonomous anaesthesia system. To continue the work it is needed to test the methods with more data in order to validate them and with some different animal species. Then an analysis of the predicted value against the anaesthetic used and its influence in the real DoA of the animal have to be modeled in order to build up a control system that predicts the variations of DoA with the anaesthetic. Then the algorithms must be integrated in a system that gives the anaesthetic drug in function of the calculated index.

In this thesis the identification of outliers was not approach, however it is a fundamental field that must be studied in order to find the periods where the signal is corrupted with noise and withdraw this unwanted signal. Moreover, with the aid of the amount of the anaesthetic drug given, a prediction of the DoA may be accomplished.

Bibliography

[1] AMIGÓ, J. & KENNEL, M. (2007). Topological permutation entropy. *Physica D*, **231**, 137–142.

[2] ASPECTMEDICAL (2010). www.aspectmedical.com.

[3] BALI, M. & AKABAS, M.H. (2004). Defining the propofol binding site location on the GABA$_a$ receptor. *Molecular Pharmacology*, **65**, 68–76.

[4] CATON, R. (1875). The Electric Currents of the Brain. *British Medical Journal*, **ii**, 278.

[5] CATON, R. (1877). Interim report on investigation of the electric currents of the brain. *British Medical Journal*, **Sumplement**, 62.

[6] CHERNIK, D., GILLINGS, D. & H. LAINE, E.A. (1990). Validity and Reliability of the Observer's: Assessment of Alertness/Sedation Scale: Study with: Intravenous Midazolam. *Journal of Clinical Psychopharmacology*, **10**, 244–251.

[7] DORLAND, W.A.N. (2007). *Dorland's Medical Dictionary*. ELSEVIER.

[8] F. G. ANTOGNINI, E.C. (2002). In vivo characterization of anaesthesia and its components. *British Journal of Anaesthesia*, **89(1)**, 156–166.

[9] FERENETS, R. & T. LIPPING, E.A. (2006). Comparison of entropy and complexity measures of the assessment of depth of sedation. *IEEE Transactions on Biomedical Engineering*, **53**, 1067–1077.

[10] GREENE, S.A. (2002). *Veterinary Anesthesia and Pain Management Secrets*. Hanley & Belfus, Inc,, Philadelphia.

[11] HUANG, J., LU, Y., NAYAK, A. & ROY, R. (2006). Depth of Anesthesia Estimation and Control. *IEEE Transactions on Biomedical Engineering*, **46(1)**, 71–81.

[12] JONES, R.S. (2001). Comparative mortality in anaesthesia. *British Journal of Anaesthesia*.

[13] JUNGE, D. (1981). *Nerve and muscle excitation*. Sinauer Associates.

[14] KANDEL, E., SCHWARTZ, J. & JESSELL, T. (2000). *Principles of Neural Science*. McGraw-Hill Medical.

[15] KKL, H., GB, M. & PENG CK, E.A. (1997). Predicting survival in heart failure case and control subjects by use of fully automated methods for deriving nonlinear and conventional indices of heart rate dynamics. *Circulation*, **96 (3)**, 842–848.

[16] KRASOWSKI, M.D., KOLTCHINE, V.V. & C. E. RICK, E.A. (1998). Propofol and other intravenous anesthetics have sites of action on the GABA receptor distinct from that for isoflurane. *Molecular Pharmacology*, **53**, 530–538.

[17] KREUER, S. & WILHELM, W. (2006). The narcotrend monitor. *Best Practice and Research. Clinical Anaesthesiology*, 111–119.

[18] M. J. GRIFFITHS, E.A., P. GRAINGER (2005). Recent advances in eeg monitoring for general anaesthesia, altered states of consciousness and sports preformance science. *3rd IEE International Seminar on Medical Applications of Signal Processing*.

[19] M. S. AVIDAN, E.A., L. ZHANG (2008). Anesthesia Awareness and the Bispectral Index. *The New England Journal of Medicine*, **358**, 1097–1108.

[20] MALMIVUO, J. & PLANSEY, R. (1995). *Bioelectromagnetism*. Oxford University Press.

[21] MORPHEUSMEDICAL (2010). www.morpheus-medical.com.

[22] NIEDERMEYER, E. & DA SILVA, F.L. (2007). *Electroencephalography: Basic Principles and Clinical Aplications*. Lippincott Williams & Wilkins.

[23] O, I., A, A. & MAZEN K, E.A. (2007). Effect of Bispectral index (BIS) monitoring on postoperative recovery and Sevoflurane consumption among morbidly obese patients undergoing laparoscopic gastric banding. *Saudi J Anaesth*, **1**, 8.

[24] OLOFSEN, E., SLEIGH, J.W. & DAHAN, A. (2008). Permutation entropy of the electroencephalogram: a measure of anaesthetic drug effect. *British Journal of Anaesthesia*, **101**, 810–821.

[25] P., G., M., B. & KEARSE L., E.A. (1997). Bispectral analysis measures sedation and memory effects of propofol, midazolam, isoflurane, and alfentanil in healthy volunteers. *Anesthesiology*, **86**, 836–847.

[26] RAMPIL, I. (1998). A Primer for EEG Signal Processing in Anesthesia. *Anesthesiology*, **89**, 980–1002.

[27] RAMSAY, M., SAVEGE, T., SIMPSON, B. & GOODWIN, R. (1974). Controlled sedation with alphaxalone-alphadolone. *British Medical Journal*, **2**, 656–659.

[28] SILVA, A., CARDOSO-CRUZ, H., SILVA, F., GALHARDO, V. & ANTUNES, L. (2010). Comparison of Anesthetic Depth Indexes Based on Thalamocortical Local Field Potentials in Rats. *Anesthesiology*, **112**, 355–363.

[29] STAWICKI, S.P. (2007). Icu corner, sedation scale: Very usefull, very underused. *OPUS 12 Scientist*, **1(2)**, 10–12.

[30] STAWICKI, S.P. (2007). Sedation scales: Very useful, very underused. *OPUS 12 Scientist*, **1(2)**, 10–12.

[31] TAKAMATSU, I., OZAKI, M. & KAZAMA, T. (2006). Entropy indices vs the bispectral index for estimating nociception during sevoflurane anaesthesia. *British Journal of Anaesthesia*, **96(5)**, 620–626.

[32] TORTORA, G.J. & GRABOWSKY, S.R. (2004). *Introduction to the Human Body*. John Wiley & Sons, Inc.

[33] TOWLE, V., BOLAÑOSA, J. & D. SUAREZA, E.A. (1993). The spatial location of EEG electrodes: locating the best-fitting sphere relative to cortical anatomy. *Electroencephalography and Clinical Neurophysiology*, **86(1)**, 1–6.

[34] ZIKOV, T., BIBIAN, S. & G. DUMONT, E.A. (2006). Quantifying Cortical Activity During General Anesthesia Using Wavelet Analysis. *IEEE Transactions on Biomedical Engineering*, **53(4)**, 617–632.

Apêndice A

Rabbits Results

In this appendix section the results obtained with the other rabbits are presented and commented.

A.0.1 Rabbit 1

In this case, the EEG signal is very corrupted with outliers.

Even though, the Index$_{BD}$, the IoC-view and the SEFBS$_{95\%}$ show a similar prediction with a higher variability in the deepest stage, coincident with a region where the signal is more corrupted, these indexes are correlated with the propofol concentration and are coherent with the clinical prediction.

The ShEn index and PE with and without the correction factor of the BSR identify the deeper level of anaesthesia.

In the comparative method the index using the five different stages makes a poor prediction to deeper stages, while the linear method using the histogram as feature do not identify intermediate states and with the frequency distribution it has problems in the identification of shallower DoA.

A.0.2 Rabbit 2

Although the quality of this acquisition is better, there is a desynchronization between the EEG data and the propofol rate. This fact can be realized due to the decrease of the Index$_{BD}$, the IoC-view and the SEFBS$_{95\%}$ simultaneously and before the indication that the infusion of the anaesthetic had started.

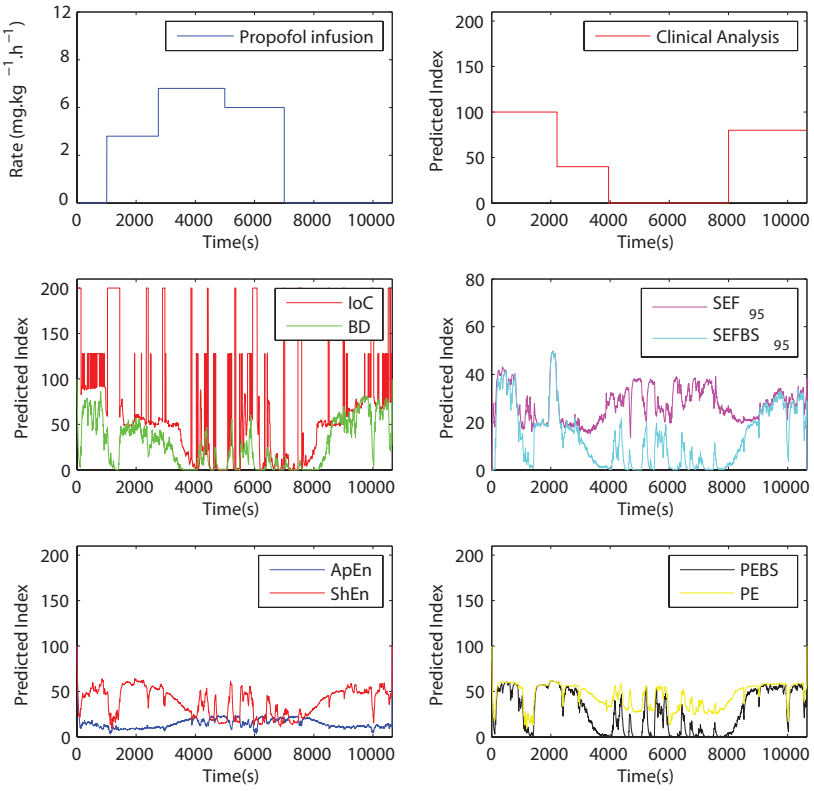

Figura A.49: Results obtained with the data acquired from the first rabbit.

In this example, the Index$_{BD}$, the IoC-view, the SEFBS$_{95\%}$ and **PEBSR!** (**PEBSR!**) have a similar evolution despite the IoC-view do not identify the deepest level while the other two indexes recognize it. The other indexes do not present any evident relation with the infusion rates or with the clinical analysis.

This time the Index$_{FSS}$ follows closely the clinical analysis, however it does not identify the deepest level. The linear method has a better performance using the frequency distribution as the feature function.

A.0.3 Rabbit 3

In this situation the signal is very corrupted again and the synchronization is not perfect.

Differently from what is seen in the clinical analysis, the Index$_{BD}$, the IoC-view and the SEFBS$_{95\%}$ show a period of time where the DoA is shallower, this epoch is relative to the reduction of the infusion rate of the propofol, around $5000s$. This event shows the subjectivity of the clinical tests

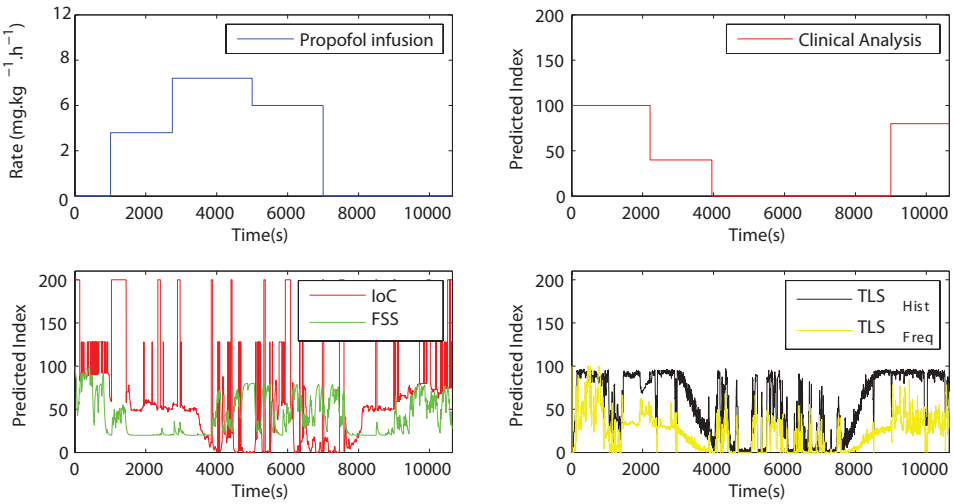

Figura A.50: Results obtained with the methods that use a database for the data acquired from the first rabbit.

while the analysis of the EEGram may prevent some cases of awareness during the procedure. These three indexes show again similar progress.

The ShEn identify different stages but it is constrained to a tight region of values. The ApEn does not point any indication of the DoA.

The comparative methods evidence the same problems and the same solution in this example as in the ones seen before.

A.0.4 Rabbit 4

In this test, the EEG signal is again affected with many periods where IoC performs some tests and the EEG is desynchronized from the clinical assessed data.

This results are coherent with the others presented previously, the Index$_{BD}$, the IoC-view and the SEFBS$_{95\%}$ still have the same course and ShEn points out the most profound stage of anaesthesia.

This example corroborates the information given in the other results.

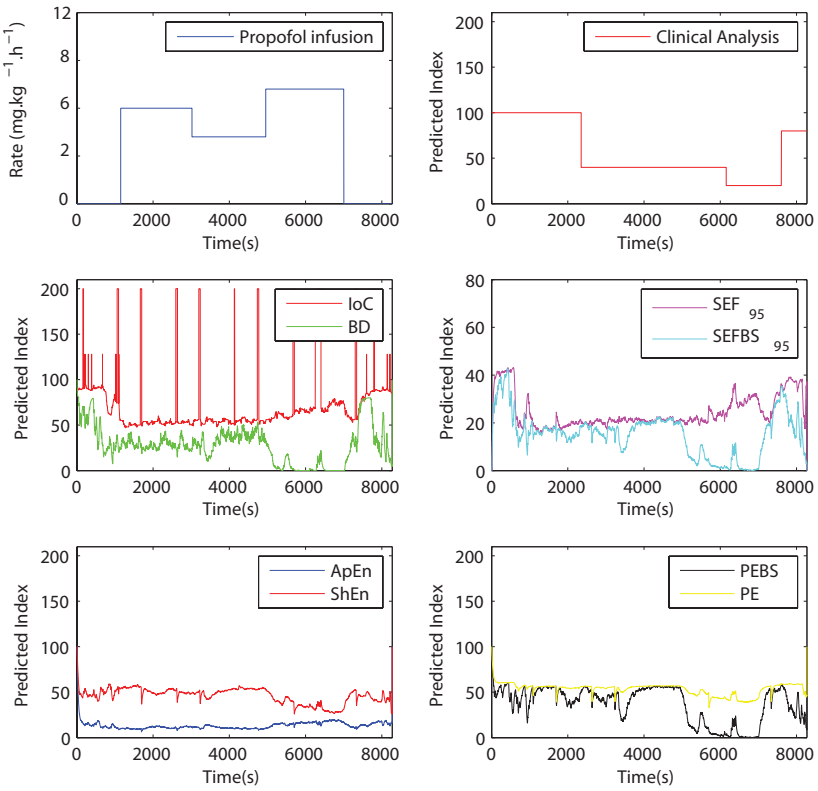

Figura A.51: Results obtained with the data acquired from the second rabbit.

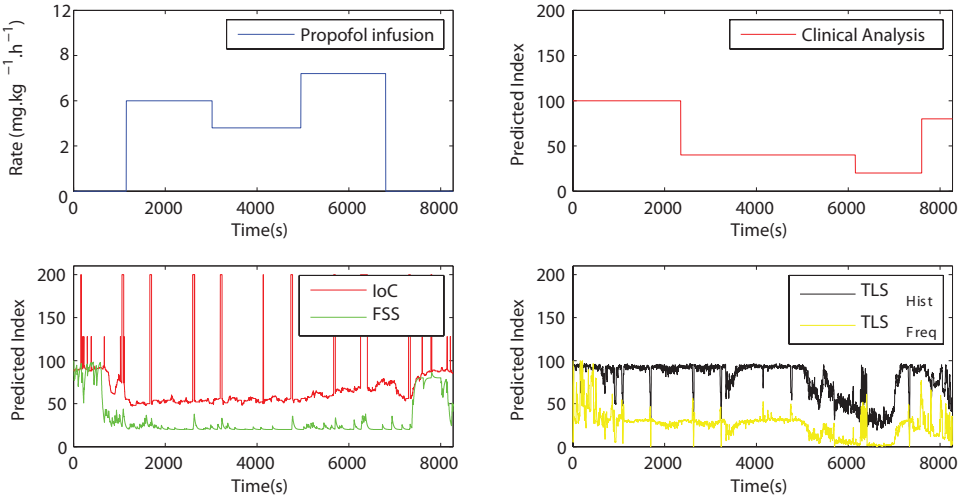

Figura A.52: Results obtained with the methods that use a database for the data acquired from the second rabbit.

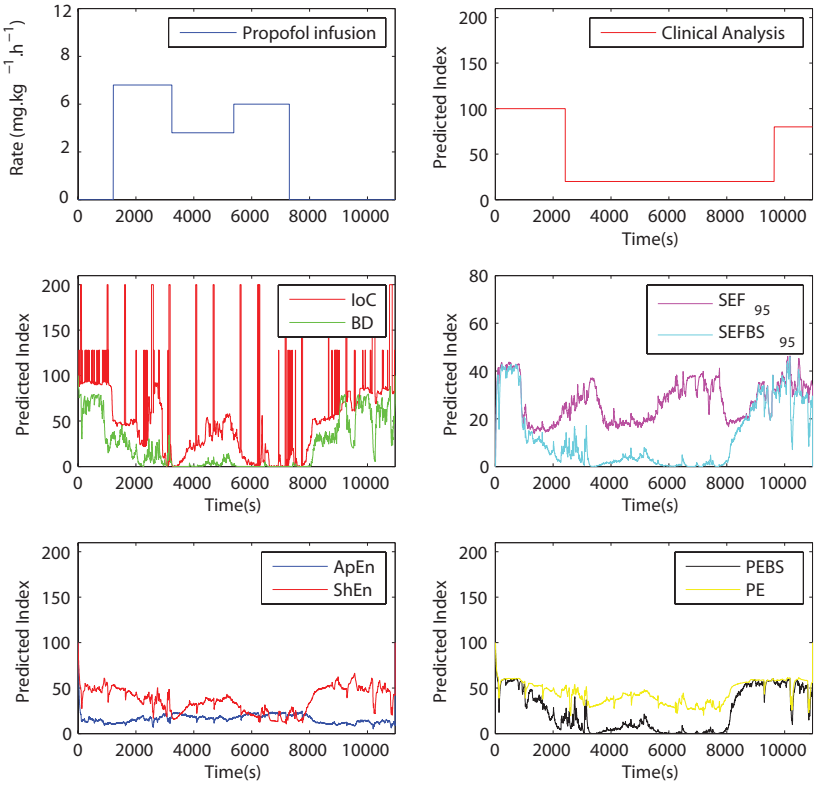

Figura A.53: Results obtained with the data acquired from the third rabbit.

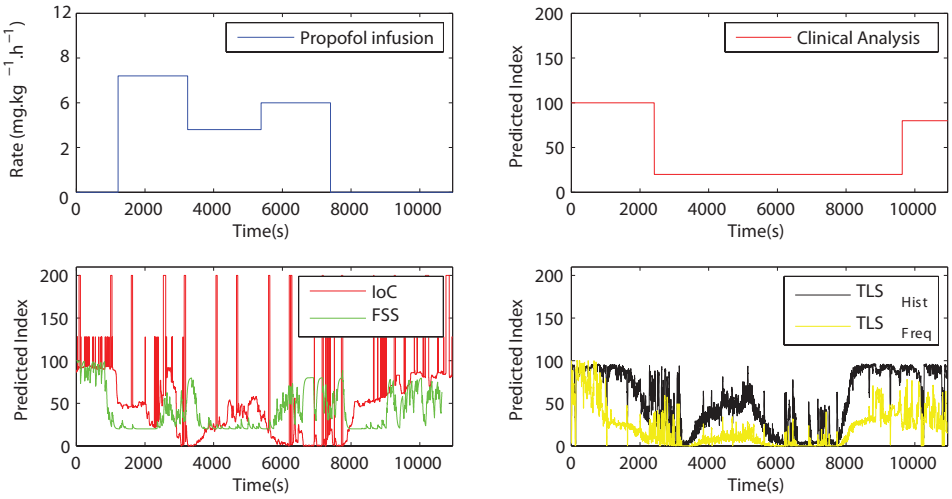

Figura A.54: Results obtained with the methods that use a database for the data acquired from the third rabbit.

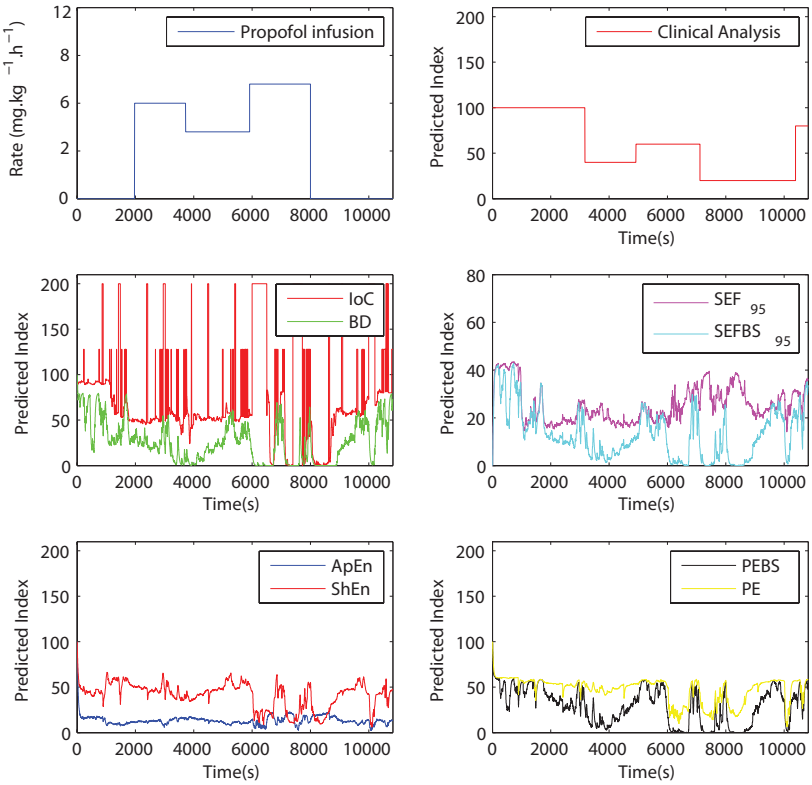

Figura A.55: Results obtained with the data acquired from the fourth rabbit.

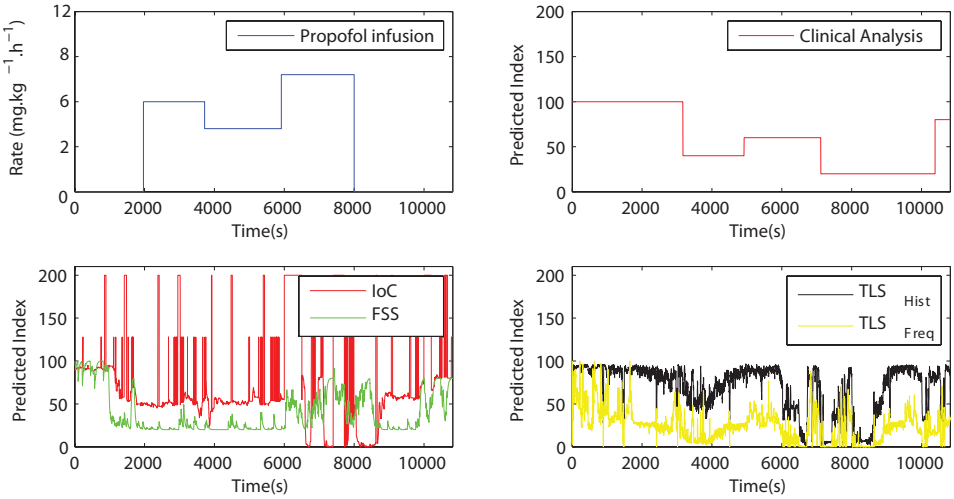

Figura A.56: Results obtained with the methods that use a database for the data acquired from the fourth rabbit.

Apêndice B

Implemented Code

B.1 Simulation

```
%% Opening data
% In this cycle the previously acquired data is selected.

% Rat

if 1

    data=open('ANA_SIVPL8_01_20080613.mat');
    animal=data.AD01-mean(data.AD01);
    Fs=500;
    limit=500;          % Defines a threshold for reasonable values
    Δ=.25*std(animal);          % Threshold value for the PE method
    ioc_emg_sqi_bs=zeros(length(animal)/500,1);
end



if 0

    data=open('coelhos_Propofol_Bertinho.mat');
    Fs=1024;
    limit=100;          % Defines a threshold for reasonable values
    Δ=.5;
end

```

```
26 % Bunny 1
27
28 if 0
29     animal=data.c11;
30     ioc_emg_sqi_bs=data.c11_ioc_emg_sqi_bs;
31     coelho_recovered=data.c11_recovered;
32
33 end
34
35 % Bunny 2
36
37 if 0
38     animal=data.c12;
39     ioc_emg_sqi_bs=data.c12_ioc_etc;
40     coelho_recovered=data.c12_recovered;
41
42
43 end
44
45 % Bunny 3
46
47 if 0
48     animal=data.c14;
49     ioc_emg_sqi_bs=data.c14_ioc_etc;
50
51 end
52
53 % Bunny 4
54
55 if 0
56     animal=data.c15;
57     ioc_emg_sqi_bs=data.c15_ioc_etc;
58     coelho_recovered=data.c15_recovered;
59
60 end
61
62 % Bunny 5
63
64 if 0
65     animal=data.c16;
66     ioc_emg_sqi_bs=data.c16_ioc_etc;
67     coelho_recovered=data.c16_recovered;
68
69 end
70
```

```
71
72 %% Filters
73 % In this step the coeficients of the filters used to separate the signal
74 % into the typical bandwidths and the filter used to remove noise are
75 % calculated.
76
77
78
79
80 % Definition of the block filter according to the EEG typical brain waves.
81 % 1-4 Hz
82 [b_Δ,a_Δ]=butter(2,[.5 4]/Fs*2);
83 % fvtool(b_Δ,a_Δ)
84
85 % 4-7 Hz
86 [b_theta,a_theta]=butter(2,[4 8]/Fs*2);
87 % fvtool(b_theta,a_theta)
88
89 % 8-12 Hz
90 [b_alpha,a_alpha]=butter(4,[8 13]/Fs*2);
91 % fvtool(b_alpha,a_alpha)
92
93 % 12-30 Hz
94 [b_beta,a_beta]=butter(5,[13 30]/Fs*2);
95 % fvtool(b_beta,a_beta)
96
97 % 30-45 Hz
98 [b_gamma,a_gamma]=butter(6,[30 45]/Fs*2);
99 % fvtool(b_gamma,a_gamma)
100
101
102
103 [b_high_pass,a_high_pass]=butter(2,.3/Fs*2,'high');
104 [b_low_pass,a_low_pass]=butter(14,45/Fs*2);
105
106 [b_high_pass_ApEn,a_high_pass_ApEn]=butter(2,.3/(Fs/4)*2,'high');
107 [b_low_pass_ApEn,a_low_pass_ApEn]=butter(14,45/(Fs/4)*2);
108
109
110
111
112 %% Vectors containing index values
113 % The vectors that store the index in order to present them after the
114 % calculation of the DoA are initialized
115
```

```
116 vect_index_BD=zeros(1,ceil(length(animal)/Fs));
117 vect_index_smooth_BD=100+zeros(1,ceil(length(animal)/Fs));
118
119
120 PE_1=zeros(1,ceil(length(animal)/Fs));
121 PE_2=zeros(1,ceil(length(animal)/Fs));
122 vect_index_PE=zeros(1,ceil(length(animal)/Fs));
123 vect_index_PE_corr_bs=zeros(1,ceil(length(animal)/Fs));
124 vect_index_smooth_PE=100+zeros(1,ceil(length(animal)/Fs));
125 vect_index_smooth_PE_corr_bs=100+zeros(1,ceil(length(animal)/Fs));
126
127 vect_index_ShEn=zeros(1,ceil(length(animal)/Fs));
128 vect_index_smooth_ShEn=100+zeros(1,ceil(length(animal)/Fs));
129
130 vect_index_ApEn=zeros(1,ceil(length(animal)/Fs));
131 vect_index_smooth_ApEn=100+zeros(1,ceil(length(animal)/Fs));
132
133 vect_index_BSR=zeros(1,ceil(length(animal)/Fs));
134
135 vect_index_SEF95=zeros(1,ceil(length(animal)/Fs));
136 vect_index_SEF95_corr_bs=zeros(1,ceil(length(animal)/Fs));
137 vect_index_smooth_SEF95=zeros(1,ceil(length(animal)/Fs));
138 vect_index_smooth_SEF95_corr_bs=zeros(1,ceil(length(animal)/Fs));
139
140 %% Temporary variables initialization
141 % Auxiliar variables used in the simulation of the real-time operation. The
142 % IoC-view sends packages of 256 samples every quarter of a second. The
143 % simulation analyzes the data acquired every second with a time window of
144 % 5 seconds.
145
146 vect_temp=zeros(1,Fs);          % Stores the 256 samples
147 vect_data=zeros(1,4*Fs/4*5);    % Stores the 5 second window
148
149 t=0;                            % Variable of time, counts the samples
150 counter=0;                      % Count the number of package recieved
151 window_N=30;                    % Window used to filter the indexes
152
153
154
155
156 %% Simulation cycle
157
158 while t/Fs+5≤floor(length(animal)/Fs)
159
160
```

```
161 %% Data aquisition
162
163
164 vect_temp(1:end-Fs/4)=vect_temp(Fs/4+1:end);
165 if Fs==1024
166     vect_temp(end-Fs/4+1:end)=900/65535*animal(t+1:t+Fs/4)-450;    % Recepção dos dados novos
167     vect_temp(end-Fs/4-1:end)=vect_temp(end-Fs/4-1:end)-mean(vect_temp(end-Fs/4-1:end));
168 else
169     vect_temp(end-Fs/4+1:end)=animal(t+1:t+Fs/4);
170 end
171
172
173
174     if counter==4               % Every four package recieved it calculates
175                                 % the index
176
177         ioc=ioc_emg_sqi_bs(t/Fs,1);     % Recieve the information sent by
178                                         % IoC-View
179
180         counter=0;                      % Reset the counter
181
182 %% Identification of outliers
183 % A simple task that tries to remove some outliers that corrupt the signal,
184 % the identification is made according to the amplitude of the signal, i.e.
185 % if the signal has an unreasonable amplitude that implies an existence of
186 % a strange sorce. The epoch corrupted with this outlier is replace by the
187 % previous epoch and so we assumed that the DoA is the same.
188
189 passador=percentil_calculator(vect_temp,limit);
190 % This function calculates the portion of the signal that is higher
191 % than the limit value.
192
193 if passador≤0
194     vect_temp=vect_temp-mean(vect_temp);
195 else
196     vect_temp=vect_data(end-Fs+1:end);
197 end
198
199 vect_temp=chauvenet_criterion(vect_temp);
200 % This step removes outliers according to chauvenet criteria.
201
202
203
204 vect_data(1:end-Fs)=vect_data(Fs+1:end);  % The data is shift
205 vect_data(end-Fs+1:end)=vect_temp;         % New data introduced
```

```
206
207
208 %% Index calculation
209
210
211
212 % The signal is filtered for the indexes that do not analyzes the
213 % distribution among the typical band wave.
214 vect_dados_filter=filter(b_low_pass,a_low_pass,vect_data);
215 vect_dados_filter=filter(b_high_pass,a_high_pass,vect_dados_filter);
216
217 % Burst Suppression Ratio
218 burstsuppression=burstsupressionQ2(vect_dados_filter,limit/10,Fs/2);
219 vect_index_BSR(t/Fs+5)=burstsuppression;
220
221 % Permutation Entropy
222 PE_1(t/Fs+5)=PE_function(vect_dados_filter,1,Δ);
223 PE_2(t/Fs+5)=PE_function(vect_dados_filter,2,Δ);
224 vect_index_PE(t/Fs+5)=100*(PE_1(t/Fs+5)+PE_2(t/Fs+5))*log(7)/log(49);
225 vect_index_smooth_PE(t/Fs+5)=...
226     (1-1/window_N)*vect_index_smooth_PE(t/Fs+5-1)...
227     +1/window_N*vect_index_PE(t/Fs+5);
228 vect_index_smooth_PE_corr_bs(t/Fs+5)=vect_index_PE(t/Fs+5)...
229     *(1-burstsuppression);
230 vect_index_smooth_PE_corr_bs(t/Fs+5)=...
231     (1-1/window_N)*vect_index_smooth_PE_corr_bs(t/Fs+5-1)...
232     +1/window_N*vect_index_smooth_PE_corr_bs(t/Fs+5);
233
234 % Shannon Entropy
235 vect_index_ShEn(t/Fs+5)=100*ShEn(vect_dados_filter,.02,limit);
236 vect_index_smooth_ShEn(t/Fs+5)=(1-1/window_N)...
237     *vect_index_smooth_ShEn(t/Fs+5-1)...
238     +1/window_N*vect_index_ShEn(t/Fs+5);
239
240 % Spectral Edge Function
241 vect_index_SEF95(t/Fs+5)=spectral_edge_frequency(vect_dados_filter,95,Fs);
242 vect_index_smooth_SEF95(t/Fs+5)=(1-1/window_N)...
243     *vect_index_smooth_SEF95(t/Fs+5-1)+1/window_N*vect_index_SEF95(t/Fs+5);
244 vect_index_SEF95_corr_bs(t/Fs+5)=vect_index_SEF95(t/Fs+5)*(1-burstsuppression);
245 vect_index_smooth_SEF95_corr_bs(t/Fs+5)=(1-1/window_N)...
246     *vect_index_smooth_SEF95_corr_bs(t/Fs+5-1)...
247     +1/window_N*vect_index_SEF95_corr_bs(t/Fs+5);
248
249 % The Aproximate Entropy is computationally heavy and so in order
250 % to reduce the workload the signal is downsample with a factor 4,
```

```
% leading to a Fs of 256.
vect_dados_ApEn=decimate(vect_temp,4);
vect_dados_ApEn=filter(b_low_pass,a_low_pass,vect_dados_ApEn);
vect_dados_ApEn=filter(b_high_pass,a_high_pass,vect_dados_ApEn);

vect_index_ApEn(t/Fs+5)=100*ApEn(vect_dados_ApEn,2,.2);
vect_index_smooth_ApEn(t/Fs+5)=(1-1/window_N)...
    *vect_index_smooth_ApEn(t/Fs+5-1)+1/window_N*vect_index_ApEn(t/Fs+5);


% Band distribution Algorithm
if burstsuppression>2/3
    vect_index_BD(t/Fs+5)=5;

elseif burstsuppression>1/3
    vect_index_BD(t/Fs+5)=4;
else

% The signal is separated into the 5 typical bands
banda_Δ=filter(b_Δ,a_Δ,vect_data);
banda_theta=filter(b_theta,a_theta,vect_data);
banda_alpha=filter(b_alpha,a_alpha,vect_data);
banda_beta=filter(b_beta,a_beta,vect_data);
banda_gamma=filter(b_gamma,a_gamma,vect_data);

% The mean power is calculated
quad_banda_Δ=banda_Δ.^2;
quad_banda_theta=banda_theta.^2;
quad_banda_alpha=banda_alpha.^2;
quad_banda_beta=banda_beta.^2;
quad_banda_gamma=banda_gamma.^2;

pot_Δ=mean(quad_banda_Δ);
pot_theta=mean(quad_banda_theta);
pot_alpha=mean(quad_banda_alpha);
pot_beta=mean(quad_banda_beta);
pot_gamma=mean(quad_banda_gamma);

vect_pot=[pot_Δ;pot_theta;pot_alpha;pot_beta;pot_gamma];
vect_pot_norm=norm(vect_pot);
vect_pot_final=vect_pot/vect_pot_norm;

% These conditions try to mimic the description found in the
% bibliography.
if vect_pot_final(3)==max(vect_pot_final)
```

```
296     vect_index_BD(t/Fs+5)=0;
297
298 elseif vect_pot_final(4)>.3
299     vect_index_BD(t/Fs+5)=1;
300
301 elseif vect_pot_final(3)+vect_pot_final(2)>.8
302     vect_index_BD(t/Fs+5)=2;
303
304 elseif vect_pot_final(1)==max(vect_pot_final)
305     vect_index_BD(t/Fs+5)=4;
306
307 elseif vect_pot_final(1)+vect_pot_final(2)>.8
308     vect_index_BD(t/Fs+5)=3;
309
310 end
311 end
312
313 vect_index_BD(t/Fs+5)=100*(1-1/5*vect_index_BD(t/Fs+5));
314 vect_index_smooth_BD(t/Fs+5)=(1-1/window_N)...
315     *vect_index_smooth_BD(t/Fs+5-1)+1/window_N*vect_index_BD(t/Fs+5);
316
317     end
318
319
320     t=t+Fs/4;
321     counter=counter+1;
322
323
324 end
```

B.2 Burst Suppression Ratio

```
1  function burst_level=burstsupressionQ2(vect_dados,threshold,tam)
2
3  %% Variables identification
4  %
5  %   vect_dados is a vector with the EEG epoch in analysis.
6  %   threshold is a constant that defines the value below which the EEG is
7  % considered isoelectric.
8  %   tam is the number of samples in an half of a second.
9
10 %%
11 vect_dados_abs=abs(vect_dados);
```

```
m=0;
burst_level=0;

for i=1:length(vect_dados_abs)

    if vect_dados_abs(i)<threshold
        m=m+1;
    elseif m>tam
        burst_level=burst_level+m;
        m=0;
    else
        m=0;
    end
end
if m>tam

    burst_level=burst_level+m;

end
burst_level=burst_level/length(vect_dados_abs);

end
```

B.3 Permutation Entropy

```
function entropy2=PE_function(vect_data,tau,Δ)

%% Variables definition
%   vect_data is the vector that has the EEG information
%   tau is space between points in the motif
%   Δ is the tolerance value
%%

entropy1=zeros(1,length(vect_data)-2*tau);

for it=1:length(vect_data)-2*tau

    if abs(vect_data(it)-vect_data(it+tau))<Δ && ...
            abs(vect_data(it+tau)-vect_data(it+2*tau))<Δ && ...
            abs(vect_data(it)-vect_data(it+2*tau))<Δ

        entropy1(it)=7;
    else
```

```
        if vect_data(it)<vect_data(it+tau)
            if vect_data(it+tau)<vect_data(it+2*tau)
                entropy1(it)=1;
            else
                if vect_data(it)<vect_data(it+2*tau)
                    entropy1(it)=2;
                else
                    entropy1(it)=3;
                end
            end
        else
            if vect_data(it+tau)>vect_data(it+2*tau)
                entropy1(it)=4;
            else
                if vect_data(it)>vect_data(it+2*tau)
                        entropy1(it)=5;
                    else
                        entropy1(it)=6;
                end
            end
        end
    end
end


p=zeros(1,7);
entropy2=0;

for intp=1:7
    p(intp)=sum(entropy1==intp)/length(entropy1);
    if p(intp)≠0
    entropy2=entropy2-(p(intp)*log(p(intp))/log(7));
    end
end

end
```

B.4 Shannon Entropy

```
function shannon_entropy=ShEn(signal,k_over_N,lim)
k_bins=k_over_N*length(signal); % Number of bins
step=((k_bins-1)/300)^-1;       % Bin interval
x_bins=-lim:step:lim;           % Vector that identifies the center of bins
```

```
vector_N=hist(signal,x_bins);    % Histogram vector
card_N=sum(vector_N);
H_Sh=0;

% Calculation of the entropy
for i=1:length(vector_N)
    if vector_N(i)≠0
    H_Sh=H_Sh-((vector_N(i)/card_N)*log((vector_N(i)/card_N)));
    end
end
shannon_entropy=H_Sh/log(k_bins);
end
```

B.5 Approximate Entropy

```
function approximate_entropy=ApEn(Sn,m,r)

%% Generation of patterns
padroes_m=cria_padroes(Sn,m);
padroes_m1=cria_padroes(Sn,m+1);

%% Calculation of the number os similar patterns with length m
cim=zeros(1,length(padroes_m));
for l=1:length(padroes_m)
nim=zeros(1,length(padroes_m));
    for i=1:length(padroes_m)
        nim(i)=compara_padroes(padroes_m{l},padroes_m{i},r);
    end
    cim(l)=sum(nim)/(length(Sn)-m+1);

end
cm=sum(cim)/(length(Sn)-m+1);

%% Calculation of the number os similar patterns with length m+1
cim1=zeros(1,length(padroes_m1));
for l=1:length(padroes_m1)
nim1=zeros(1,length(padroes_m1));
    for i=1:length(padroes_m1)
        nim1(i)=compara_padroes(padroes_m1{l},padroes_m1{i},r);

    end

    cim1(l)=sum(nim1)/(length(Sn)-m);
```

```
end
cm1=sum(cim1)/(length(Sn)-m);
approximate_entropy=log(cm/cm1);
end

%% Auxiliar functions

function padroes=cria_padroes(Sn,m)
padroes={};
for index=1:length(Sn)-m-1
    padroes{index}=Sn(index:index+m);
end
end

function semelhanteQ=compara_padroes(pi,pj,r)
semelhanteQ=0;
for k=1:length(pi)
    if abs(pi(k)-pj(k))>r
        return
    end
end
semelhanteQ=1;
end
```

B.6 Spectral Edge Frequency

```
function frequency=spectral_edge_frequency(signal,perc_pot,Fs)

dimension=size(signal);
if dimension(2)≠1
    signal=signal';
end
L = length(signal);

% Calculation of the Fourier Transfomr
Y_pot = fft(signal,L*2);

% Calculation of the Power Spectrum
pot_fft=Y_pot(1:L)'*Y_pot(1:L);
f = Fs/2*linspace(0,1,L);
increment=1;

if perc_pot>1
```

```
18      pot_wanted=pot_fft*perc_pot/100;
19  else
20      pot_wanted=pot_fft*perc_pot;
21  end
22
23  index=find(max(signal),1,'last');
24  pot_parcial=Y_pot(1:index)'*Y_pot(1:index);
25
26  % Identification of the SEF
27  if pot_parcial< pot_wanted
28      while pot_parcial < pot_wanted
29          index=index+increment;
30          pot_parcial=Y_pot(1:index)'*Y_pot(1:index);
31      end
32  else
33      while pot_parcial < pot_wanted
34          index=index-increment;
35          pot_parcial=Y_pot(1:index)'*Y_pot(1:index);
36      end
37  end
38  frequency=f(index);
39  end
```